NASA TECHNICAL MEMORANDUM

UB
NASA TM X-1332

UB NASA TM X-1332

AERODYNAMIC CHARACTERISTICS AT MACH NUMBERS OF 3.95 AND 4.63 FOR A MISSILE MODEL HAVING ALL-MOVABLE WINGS AND INTERDIGITATED TAILS

by M. Leroy Spearman and William A. Corlett

Langley Research Center

Langley Station, Hampton, Va.

NATIONAL AERONAUTICS AND SPACE ADMINISTRATION • WASHINGTON, D. C. • JANUARY 1967

AERODYNAMIC CHARACTERISTICS AT MACH NUMBERS OF 3.95 AND 4.63 FOR A MISSILE MODEL HAVING ALL-MOVABLE WINGS AND INTERDIGITATED TAILS

By M. Leroy Spearman and William A. Corlett

Langley Research Center
Langley Station, Hampton, Va.

NATIONAL AERONAUTICS AND SPACE ADMINISTRATION

~~CONFIDENTIAL~~

AERODYNAMIC CHARACTERISTICS AT MACH NUMBERS OF 3.95 AND 4.63 FOR A MISSILE MODEL HAVING ALL-MOVABLE WINGS AND INTERDIGITATED TAILS*

By M. Leroy Spearman and William A. Corlett
Langley Research Center

SUMMARY

A study has been made of a cruciform missile configuration having all-movable wing controls and interdigitated tails. The configuration was tested with the wings in the vertical and horizontal planes (roll angle of 0^{o}) and with the wings in a 45^{o} roll plane. Results are presented for Mach numbers of 3.95 and 4.63 and are summarized with results of a previous study at Mach numbers from 0.40 to 2.86.

The results indicate that the all-movable wings are capable of providing positive control effectiveness in pitch, yaw, and roll. In general, the control effectiveness at low angles of attack decreased with increasing Mach number but increased at high angles of attack particularly at the higher Mach numbers. The cross-control characteristics between roll and yaw were adverse at high angles of attack, however.

Only a slight forward movement of the aerodynamic center occurred with increasing supersonic Mach number near zero angle of attack. With increasing angle of attack, however, a pitch-up tendency was indicated for the configuration in the 45^{o} roll attitude.

INTRODUCTION

One of the aerodynamic requirements for ground-to-air and air-to-air missiles is the ability to attain large changes in flight-path angle that are necessary for target acquisition at supersonic or hypersonic speeds. The aerodynamic characteristics of various missile configurations considered for intercept missions have been investigated by the National Aeronautics and Space Administration and some of the results are presented in references 1 to 9.

Configurations contained in the references include several control concepts and arrangements such as canard controls, aft tails, all-movable wings, and wing trailing-edge flaps. One arrangement (ref. 7) compares the effects of an all-movable wing control

*Title, Unclassified.

and an all-movable aft tail control on a cruciform missile. As a continuation of the study of various missile arrangements, the present investigation is concerned with an arrangement having all-movable interdigitated cruciform wing controls and fixed cruciform tails.

Results presented herein were obtained in the Langley Unitary Plan wind tunnel at Mach numbers of 3.95 and 4.63. Some of these results are summarized with results obtained from reference 9 for the same configuration at Mach numbers from 0.40 to 2.86.

SYMBOLS

The results are referred to the body-axis system except for the lift and drag characteristics which are referred to the stability-axis system. The moments are referred to a point on the model center line located at 59.8 percent of the body length.

The units used for the physical quantities defined in this paper are given both in U.S. Customary Units and in the International System of Units (SI). Factors relating the two systems are given in reference 10.

A reference area, $\pi d^2/4$

d reference length, base diameter

C_A axial-force coefficient, $\frac{\text{Axial force}}{qA}$

$C_{A,c}$ chamber axial-force coefficient, $\frac{\text{Chamber axial force}}{qA}$

C_D drag coefficient, $\frac{\text{Drag}}{qA}$

$C_{D,o}$ drag coefficient at $\alpha = 0^o$

C_L lift coefficient, $\frac{\text{Lift}}{qA}$

C_{L_α} lift-curve slope, $\alpha = 0^o$

C_l rolling-moment coefficient, $\frac{\text{Rolling moment}}{qAd}$

C_{l_δ} rolling-moment coefficient due to control deflection

C_m pitching-moment coefficient, $\frac{\text{Pitching moment}}{qAd}$

C_{m_α} slope of pitching-moment curve, $\alpha = 0^\circ$

C_{m_δ} pitching-moment coefficient due to control deflection at $\alpha = 0^\circ$, per degree

C_N normal-force coefficient, $\frac{\text{Normal force}}{qA}$

C_n yawing-moment coefficient, $\frac{\text{Yawing moment}}{qAd}$

C_{n_β} variation of yawing moment with sideslip, per degree

C_{n_δ} yawing-moment coefficient due to control deflection

C_Y side-force coefficient, $\frac{\text{Side force}}{qAd}$

C_{Y_β} variation of side force with sideslip, per degree

L/D lift-drag ratio

l body length

M Mach number

q free-stream dynamic pressure

x_{ac} longitudinal distance from nose to aerodynamic center

x_{cg} longitudinal distance from nose to reference center of gravity

α angle of attack, degrees

β angle of sideslip, degrees

δ control deflection, degrees

ϕ angle of wing-chord plane with respect to lateral reference plane in model, degrees

Components:

B body

T tails

W wings

APPARATUS AND TESTS

Tunnel

The investigation was conducted in the high Mach number test section of the Langley Unitary Plan wind tunnel which is a variable-pressure continuous flow tunnel. The test section is of the asymmetric sliding-block type which permits a continuous variation in test-section Mach number from about 2.3 to 4.7.

Model

Details of the model are shown in figure 1 and geometric characteristics are given in table I. A photograph of the model is presented in figure 2. The model is the same as the booster-off model of reference 9.

The model consisted of a forebody attached by means of a 11.5° flare to a larger cylindrical afterbody. The model was equipped with fixed cruciform tails located at the model base and all-movable cruciform wings. The tail and wing surfaces had hexagonal sections at an angle 20° normal to the leading and trailing edges. The wing and tail surfaces were spaced circumferentially at 45° intervals with respect to each other. Provision was made so that the model could be mounted in the tunnel with the wing-chord plane at a roll angle of 0° or 45° relative to the lateral plane in the model.

Tests

The conditions under which the tests were conducted are as follows:

Mach number	Stagnation pressure		Stagnation temperature	
	lb/sq ft	kN/m^2	$^{\circ}F$	$^{\circ}K$
3.95	4800	230.0	175	353
4.63	6575	315.0	175	353

The Reynolds number was 2.5×10^6 per foot (per 30.5 cm). The dewpoint, measured at stagnation pressure, was maintained below -30° F (-34° C) to assure negligible condensation effects. The angle of attack was varied from approximately -6° to 21° at an angle of sideslip of 0°, and the sideslip angle was varied from about -4° to 8° at angles of attack of about 0°, 8°, and 20°. In order to fix the location of boundary-layer transition, 1/16-inch-wide (0.0016-cm) strips of No. 60 carborundum grit were placed 0.4 inch (0.01 cm) aft on the wings and tails (measured streamwise) and on the body 0.75 inch (0.019 cm) aft of the nose.

Measurements

Aerodynamic forces and moments on the model were measured by means of a six-component electrical strain-gage balance which was housed within the model. The balance was attached to a sting which, in turn, was rigidly fastened to the tunnel support system. Balance-chamber pressure was measured by means of a single static-pressure orifice located in the vicinity of the balance.

CORRECTIONS AND ACCURACY

The angles of attack and sideslip have been corrected for deflection of the balance and sting due to aerodynamic loads; angles of attack have also been corrected for tunnel airflow misalinement. The results have been adjusted to correspond to free-stream static pressure acting over the model base. The chamber axial-force coefficients are presented in figure 3.

Based on balance calibration and data repeatability, the present data are estimated to be accurate to within the following limits:

C_A, C_D	±0.025
C_N, C_L	±0.076
C_m	±0.057
C_n	±0.029
C_l	±0.010
C_Y	±0.029
M (3.95 and 4.63)	±0.050
α, deg	±0.1
β, deg	±0.1

PRESENTATION OF RESULTS

The results of the investigation are presented as follows:

DISCUSSION

Longitudinal Aerodynamic Characteristics

The results for various component arrangements (figs. 4 and 5) indicate reasonably linear variations of C_N, C_L, and C_m with α for both Mach numbers and both roll angles. The results for various pitch-control deflections of the wings (figs. 6 and 7) indicate a destabilizing contribution of the wings at $\phi = 45^{\circ}$ that becomes more pronounced as the wings are deflected. In addition, the variation of C_m with α becomes more nonlinear than at $\phi = 0^{\circ}$. The pitch-control effectiveness indicates an increase with increasing angle of attack for both roll angles. Presumably this increase in effectiveness occurs partly because of an increase in local dynamic pressure on the compression side of the wings, particularly for $\phi = 0^{\circ}$, and partly because of a loss in tail moment at $\phi = 45^{\circ}$ caused by wing induced interference.

A summary of the variation of some of the longitudinal parameters with Mach number as measured near $\alpha = 0^{\circ}$ is presented in figure 8. These results include those presented in reference 9 for the Mach number range from 0.40 to 2.86. The variations of C_{m_δ}, and $C_{D,o}$ and C_{L_α} with Mach number are typical of what might be expected. The lower values of C_{m_δ} for $\phi = 0^{\circ}$ result because only two wings are deflected in this case whereas all four wings are deflected for $\phi = 45^{\circ}$. The aerodynamic center location indicates a slight forward movement with increasing supersonic Mach number. Such a movement should be compatible with the flight center-of-gravity variation which would generally be expected to move forward with increasing Mach number while fuel is being consumed.

The pitch-control results presented herein have been used together with the results contained in reference 9 to relate the basic aerodynamic characteristics to the maneuvering capabilities of the configuration. The results (fig. 9) show the variation of trimmed C_L with Mach number for various positions of the center of gravity for the configuration at $\phi = 45^{\circ}$ and 0° and for a maximum pitch-control deflection of 25°. The results reflect the general increase in trimmed C_L that is expected as the center of gravity is moved rearward and the stability margin is decreased. These results are restricted to conditions of positive static stability only and are terminated when a nonlinear pitching-moment variation results in the occurrence of more than one trim point.

At a Mach number of 1.5, the variation of trimmed C_L with center-of-gravity position is relatively small because of the generally higher levels of static stability and the more linear variations of C_{m_α} and C_{m_δ}. With increasing Mach number the values of trimmed C_L initially tend to decrease primarily because of the decrease in C_{m_δ}. With further increase in Mach number, the values of trimmed C_L tend to increase for a given center-of-gravity position and to become much more sensitive to variations in the center of gravity. The tendency toward higher available values of trimmed lift at higher Mach numbers results, in general, from a combination of the reduction in stability level and the increase in C_{m_δ} at high angles of attack. The more nonlinear pitching-moment variation for $\phi = 45^{\circ}$ requires a more forward center-of-gravity position and results in lower values of trimmed C_L at the highest Mach number before the onset of static instability.

Lateral Control Characteristics

The effects of differential deflection of all four wing panels for roll control are presented in figure 10 for $\phi = 45^{\circ}$ and in figure 11 for $\phi = 0^{\circ}$. A high degree of roll effectiveness is indicated for both roll angles and the effectiveness increases with increasing angle of attack. The yawing moment produced, however, becomes increasingly adverse with increasing angle of attack. Results are shown in figure 12 for $\phi = 45^{\circ}$

where only two wing panels (upper left and lower right) are deflected differentially. The results, in general, are similar to those for all four wings deflected (fig. 10) except that the increments in C_l and C_n are reduced by about one-half.

The effects of yaw-control deflection are shown in figure 13 for $\phi = 45^\circ$ (four wings deflected) and in figure 14 for $\phi = 0^\circ$ (vertical wings only deflected). The results in both cases indicate a positive yaw effectiveness that increases with increasing angle of attack together with an adverse rolling moment.

The variations of the roll- and yaw-control effectiveness parameters with Mach number for $\alpha = 0^\circ$ are shown in figure 15.

Sideslip Characteristics

The variations of the aerodynamic characteristics with angle of sideslip are presented for three angles of attack in figure 16 for $\phi = 45^\circ$ and in figure 17 for $\phi = 0^\circ$. These results indicate only slight effects of sideslip on C_m, C_A, and C_N for either roll angle. Relatively little directional stability is indicated for the moment reference center used although the magnitude of the side-force variation with β indicates that some directional stability would be realized for further forward locations of the center of gravity. A substantial amount of induced roll is indicated for the highest angle of attack (20.4°) – the variation in rolling moment with β being negative at $\phi = 45^\circ$ and positive at $\phi = 0^\circ$.

The variation of C_{n_β} and C_{Y_β} with Mach number for $\alpha = 0^\circ$ is shown in figure 18.

CONCLUDING REMARKS

A study has been made of a cruciform missile configuration having all-movable wing controls and interdigitated tails. The configuration was tested with the wings in the vertical and horizontal planes (roll angle of 0°) and with the wings in a 45° roll plane. Results are presented for Mach numbers of 3.95 and 4.63 and are summarized with results of a previous study at Mach numbers from 0.40 to 2.86.

The results indicate that the all-movable wings are capable of providing positive control effectiveness in pitch, yaw, and roll. In general, the control effectiveness at low angles of attack decreased with increasing Mach number but increased at high angles of attack particularly at the higher Mach numbers. The cross-control characteristics between roll and yaw were adverse at high angles of attack, however.

Only a slight forward movement of the aerodynamic center occurred with increasing supersonic Mach number near zero angle of attack. With increasing angle of attack, however, a pitch-up tendency was indicated for the configuration in the 45° roll attitude.

Langley Research Center,
National Aeronautics and Space Administration,
Langley Station, Hampton, Va., September 29, 1966,
126-13-02-01-23.

REFERENCES

1. Stone, David G.: Maneuver Performance of Interceptor Missiles. NACA RM L58E02, 1958.

2. Robinson, Ross B.: Wind-Tunnel Investigation at a Mach Number of 2.01 of the Aerodynamic Characteristics in Combined Angles of Attack and Sideslip of Several Hypersonic Missile Configurations With Various Canard Controls. NACA RM L58A21, 1958.

3. Spearman, M. Leroy; and Robinson, Ross B.: Longitudinal Stability and Control Characteristics at Mach Numbers of 2.01, 4.65, and 6.8 of Two Hypersonic Missile Configurations, One Having Low-Aspect-Ratio Cruciform Wings With Trailing-Edge Flaps and One Having a Flared Afterbody and All-Movable Controls. NASA TM X-46, 1959.

4. Robinson, Ross B.; and Bernot, Peter T.: Aerodynamic Characteristics at a Mach Number of 6.8 of Two Hypersonic Missile Configurations, One With Low-Aspect-Ratio Cruciform Fins and Trailing-Edge Flaps and One With a Flared Afterbody and All-Movable Controls. NACA RM L58D24, 1958.

5. Turner, Kenneth L.; and Appich, W. H., Jr.: Investigation of the Static Stability Characteristics of Five Hypersonic Missile Configurations at Mach Numbers From 2.29 to 4.65. NACA RM L58D04, 1958.

6. Church, James D.; and Kirkland, Ida M.: Static Aerodynamic Characteristics of Several Hypersonic Missile-and-Control Configurations at a Mach Number of 4.65. NASA TM X-187, 1960.

7. Robinson, Ross B.; and Foster, Gerald V.: Static Longitudinal Stability and Control Characteristics at a Mach Number of 2.01 of a Hypersonic Missile Configuration Having All-Movable Wing and Tail Surfaces. NASA TM X-516, 1961.

8. Fuller, Dennis E.; and Corlett, William A.: Supersonic Aerodynamic Characteristics of a Cruciform Missile Configuration With Low-Aspect-Ratio Wings and In-Line Tail Controls. NASA TM X-1025, 1964.

9. Foster, Gerald V.; and Corlett, William A.: Aerodynamic Characteristics at Mach Numbers From 0.40 to 2.86 of a Missile Model Having All-Movable Wings and Interdigitated Tails. NASA TM X-1184, 1965.

10. Mechtly, E. A.: The International System of Units – Physical Constants and Conversion Factors. NASA SP-7012, 1964.

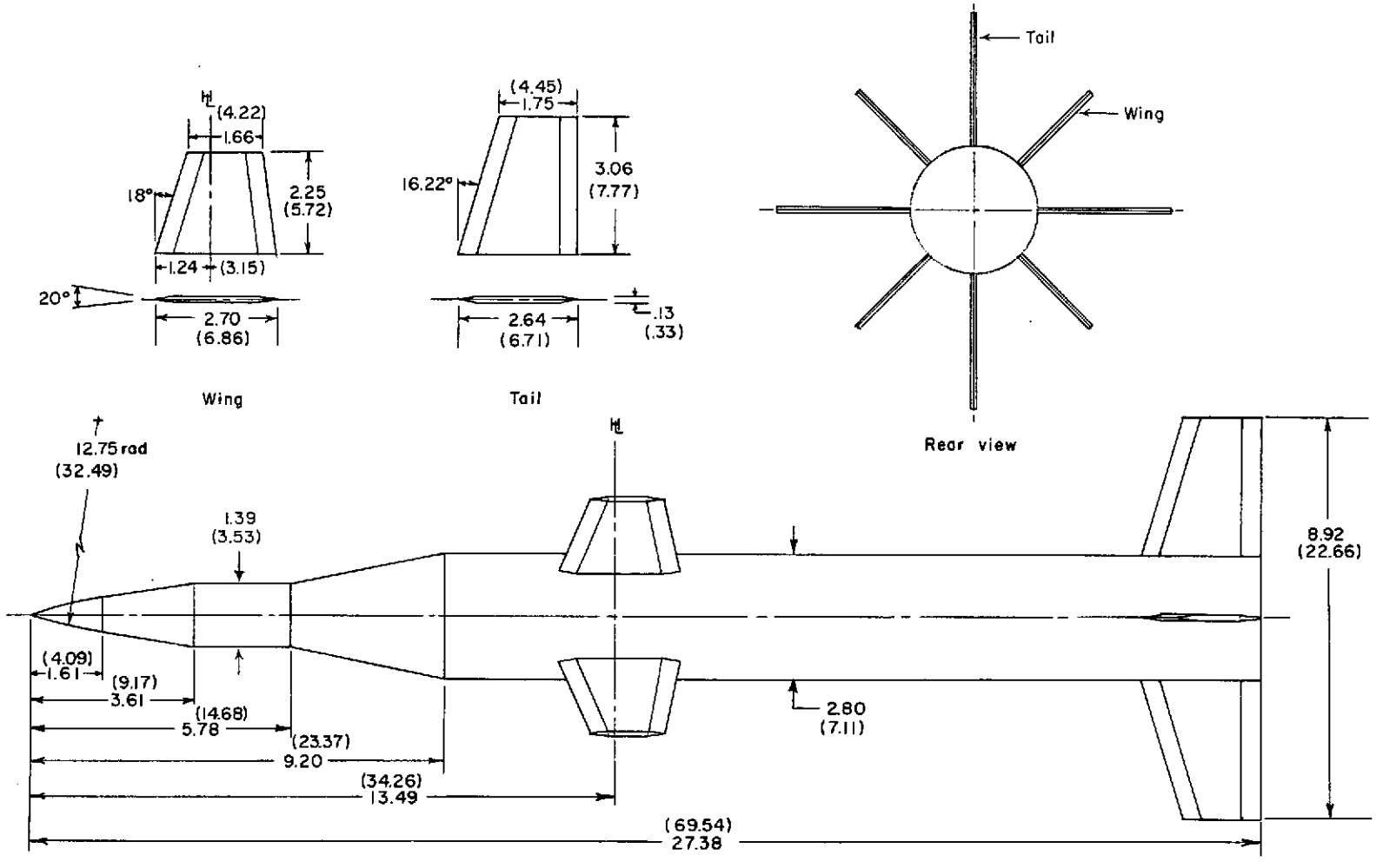

Figure 1.- Details of model. Linear dimensions are in inches (values within parentheses are in centimeters).

TABLE I.- GEOMETRIC CHARACTERISTICS OF MODEL

Body:		
Maximum diameter	2.80 in.	(7.11 cm)
Length	27.38 in.	(69.55 cm)
Base area	6.16 sq in.	(39.74 sq cm)
Wing:		
Maximum span	7.30 in.	(18.54 cm)
Tip chord	1.66 in.	(4.22 cm)
Root chord (at body juncture)	2.70 in.	(6.86 cm)
Area (each)	4.91 sq in.	(31.68 sq cm)
Sweep angle of leading edge	18.0^{o}	
Tail:		
Maximum span	8.92 in.	(22.66 cm)
Tip chord	1.75 in.	(4.45 cm)
Root chord (at body juncture)	2.64 in.	(6.71 cm)
Area (each)	6.72 sq in.	(43.35 sq cm)
Sweep angle of leading edge	16.22^{o}	

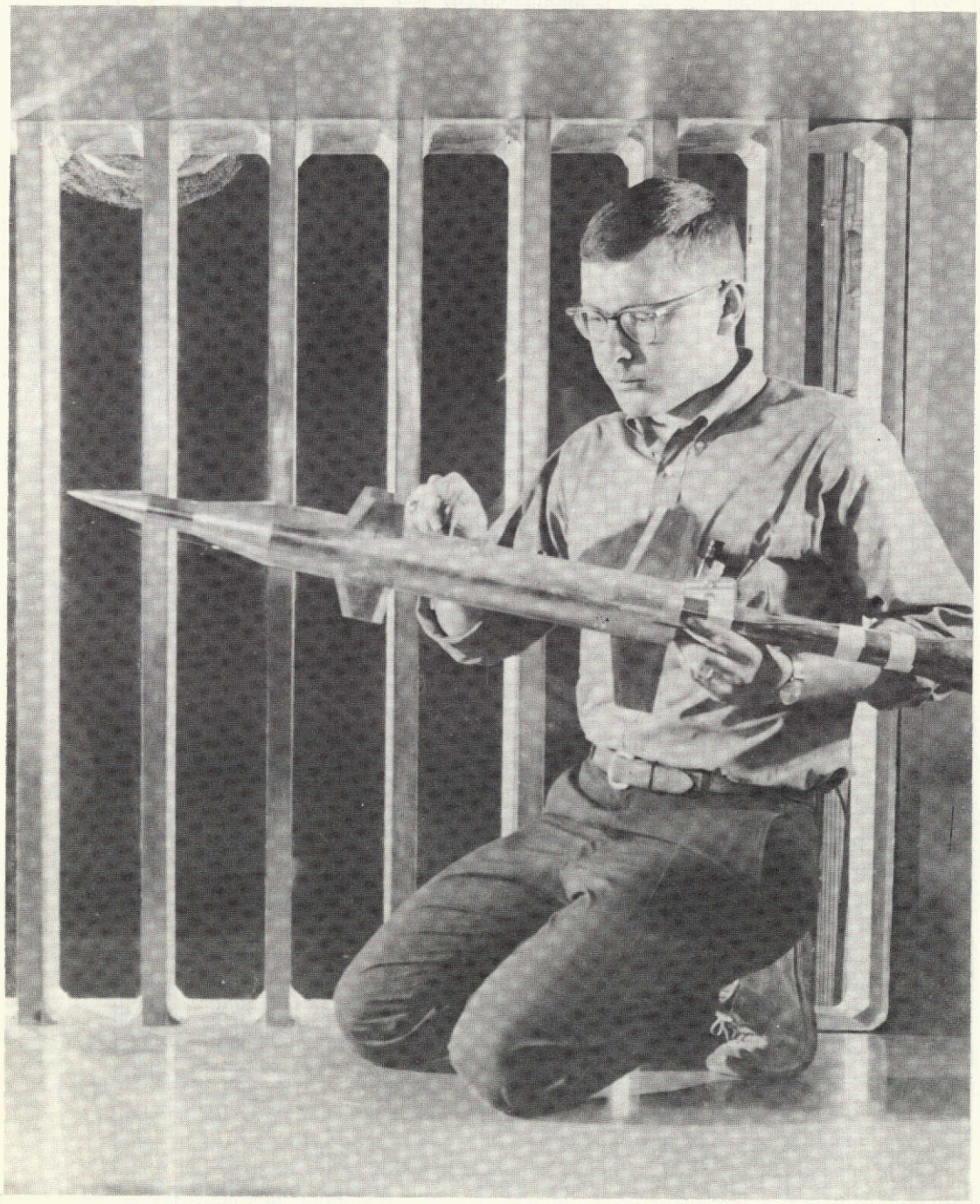

Figure 2.- Photograph of model. L-66-1934

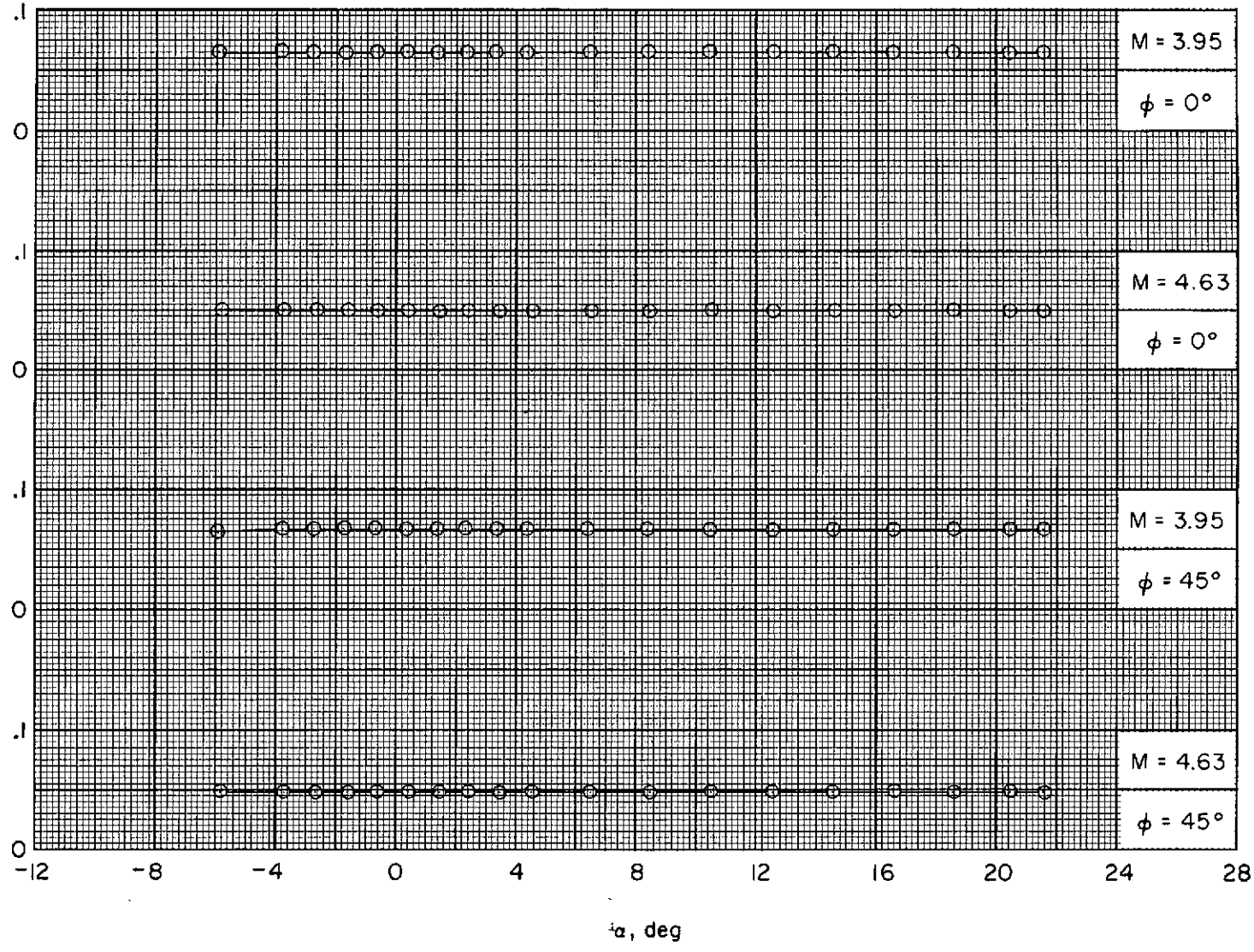

Figure 3.- Chamber axial-force coefficients.

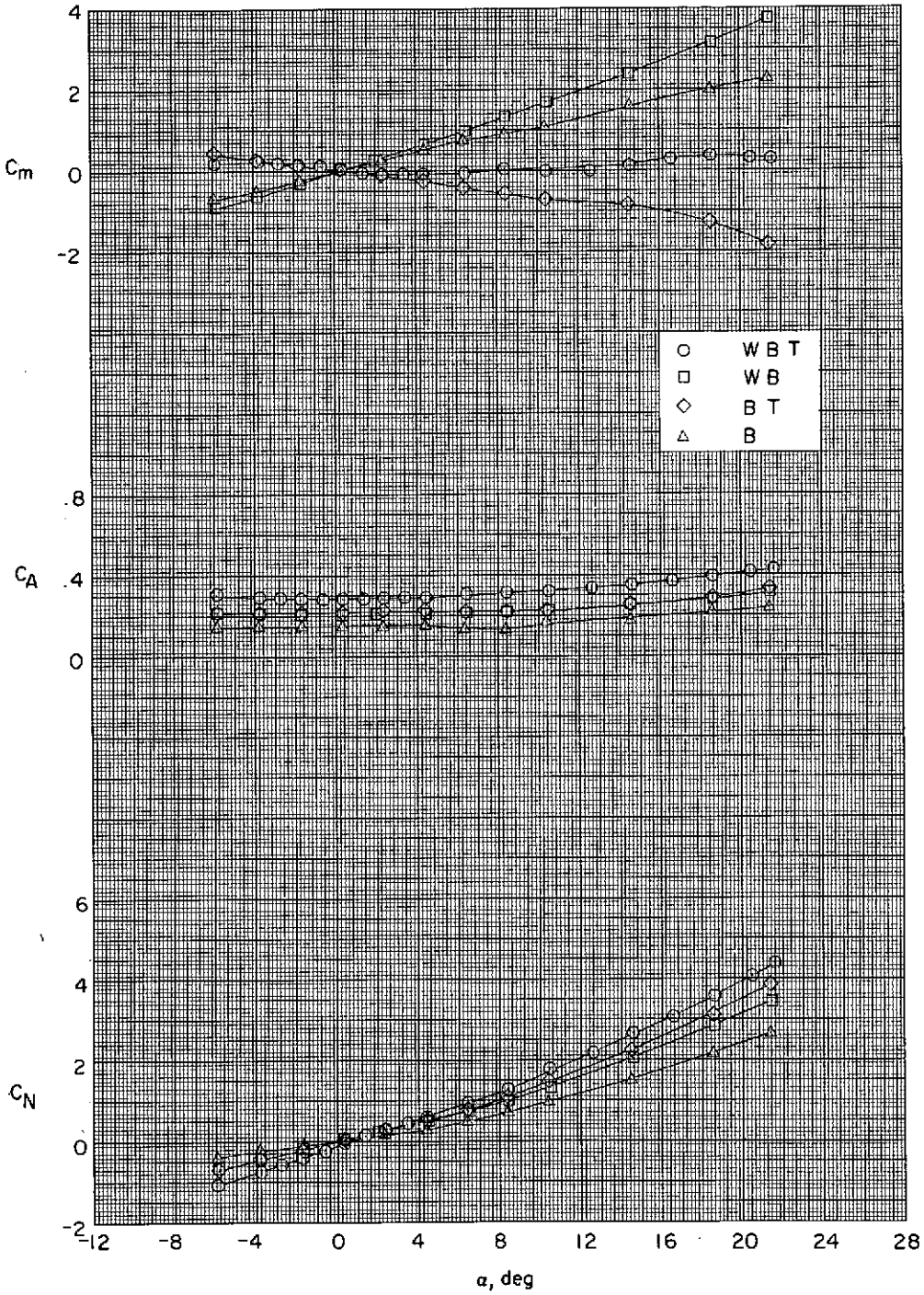

(a) M = 3.95.

Figure 4.- Longitudinal characteristics for various configuration components; $\Phi = 45^{o}$.

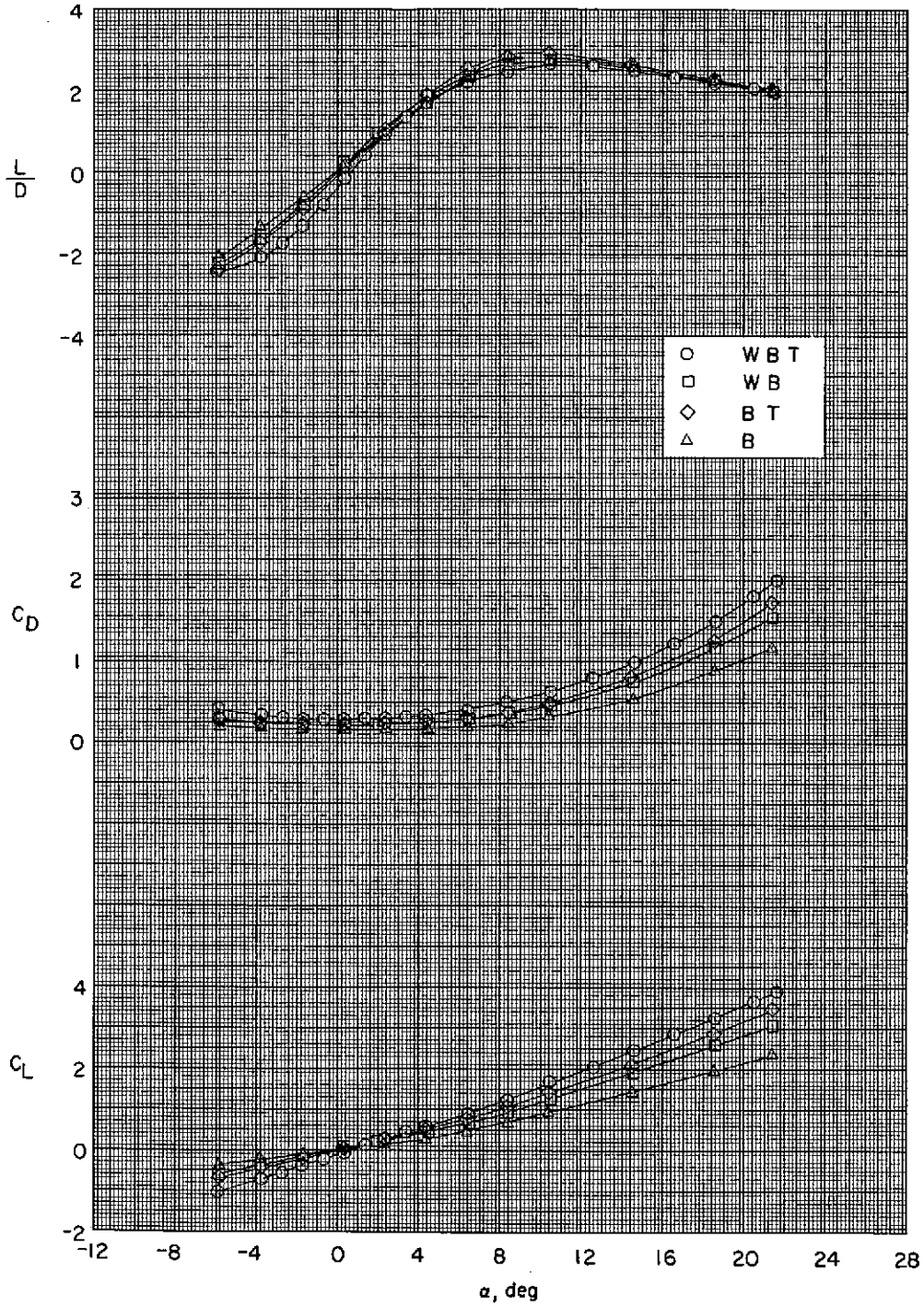

(a) Concluded.

Figure 4.- Continued.

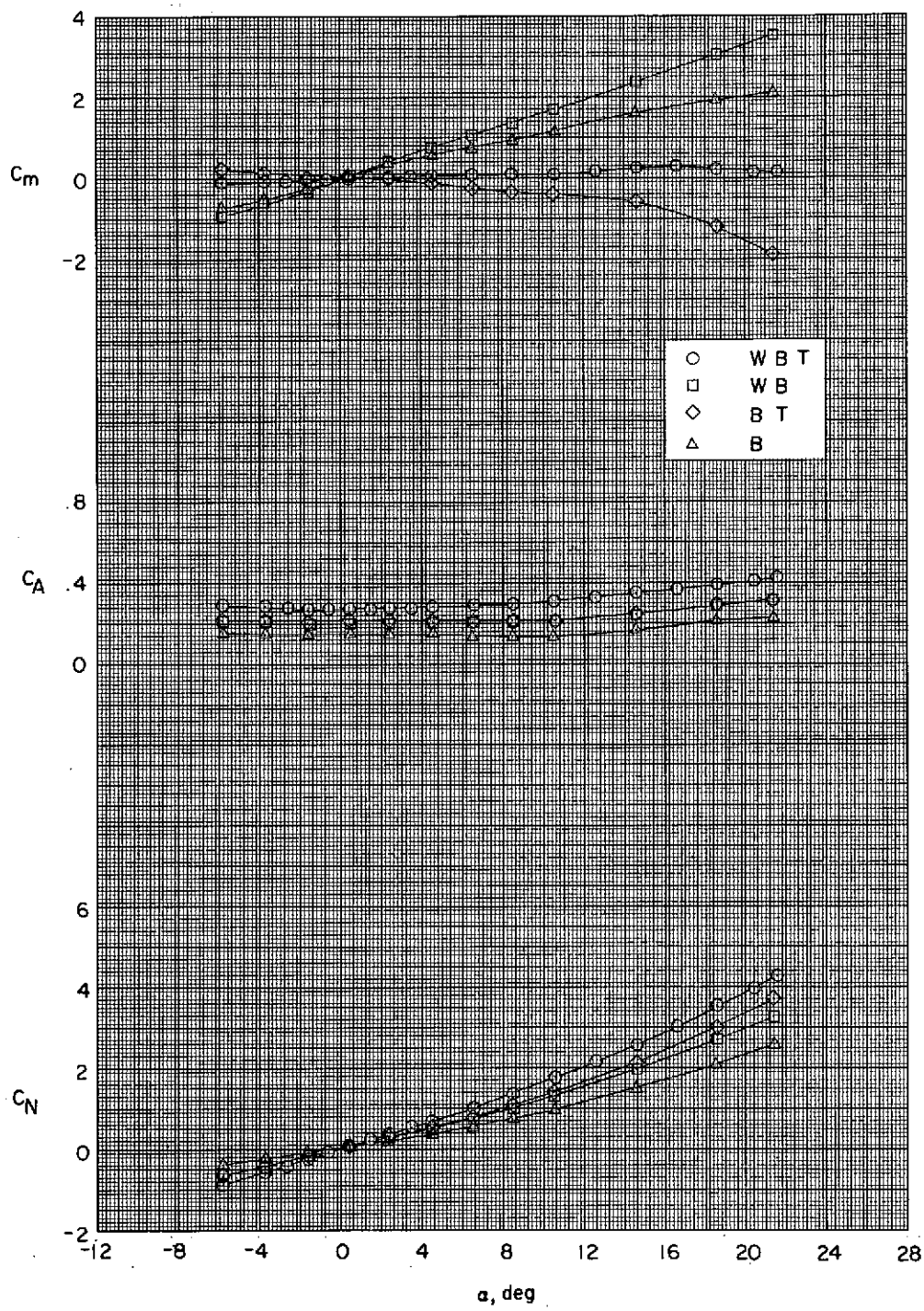

(b) M = 4.63.

Figure 4.- Continued.

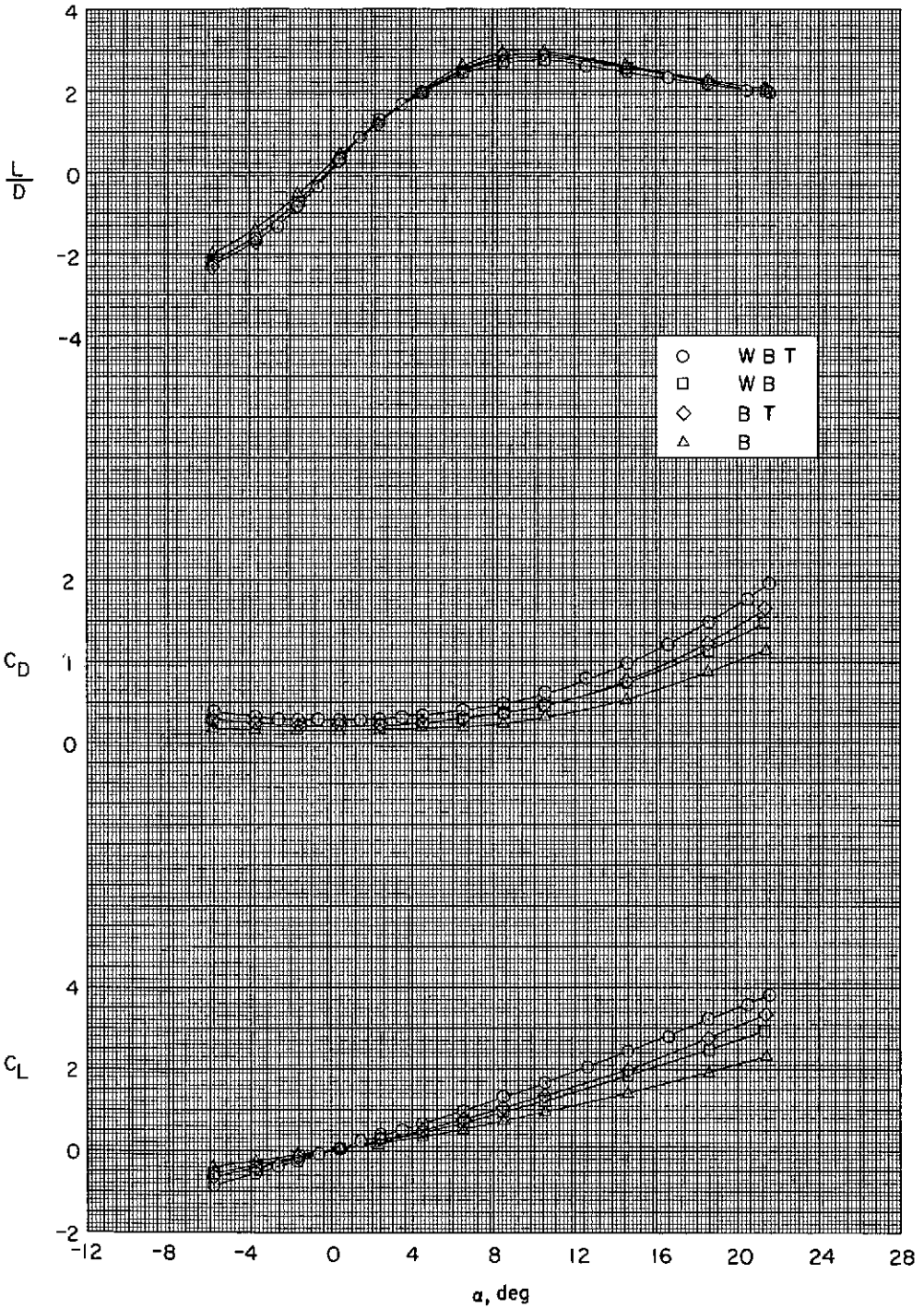

(b) Concluded.

Figure 4.- Concluded.

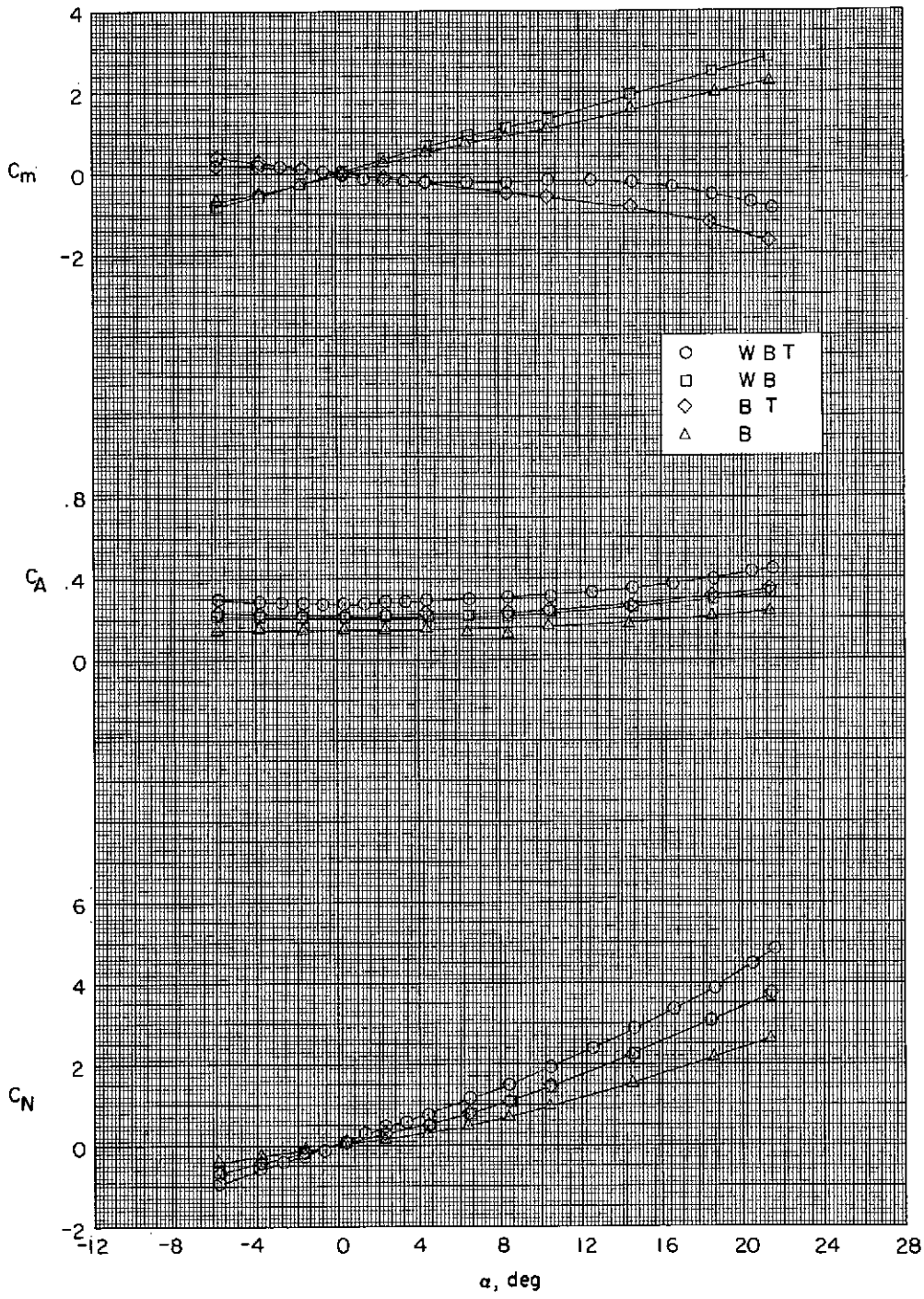

(a) M = 3.95.

Figure 5.- Longitudinal characteristics for various configuration components; $\Phi = 0^{o}$.

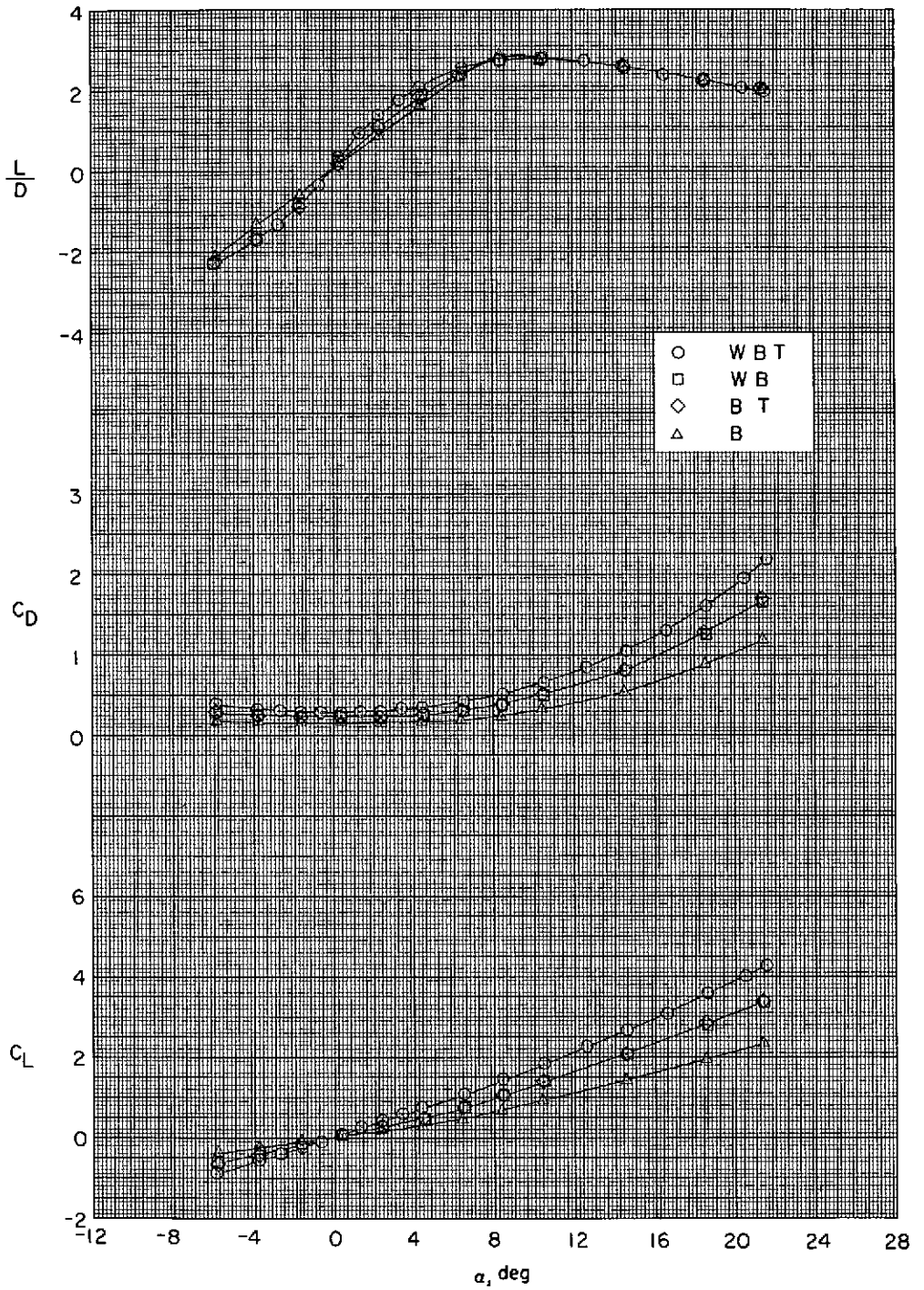

(a) Concluded.

Figure 5.- Continued.

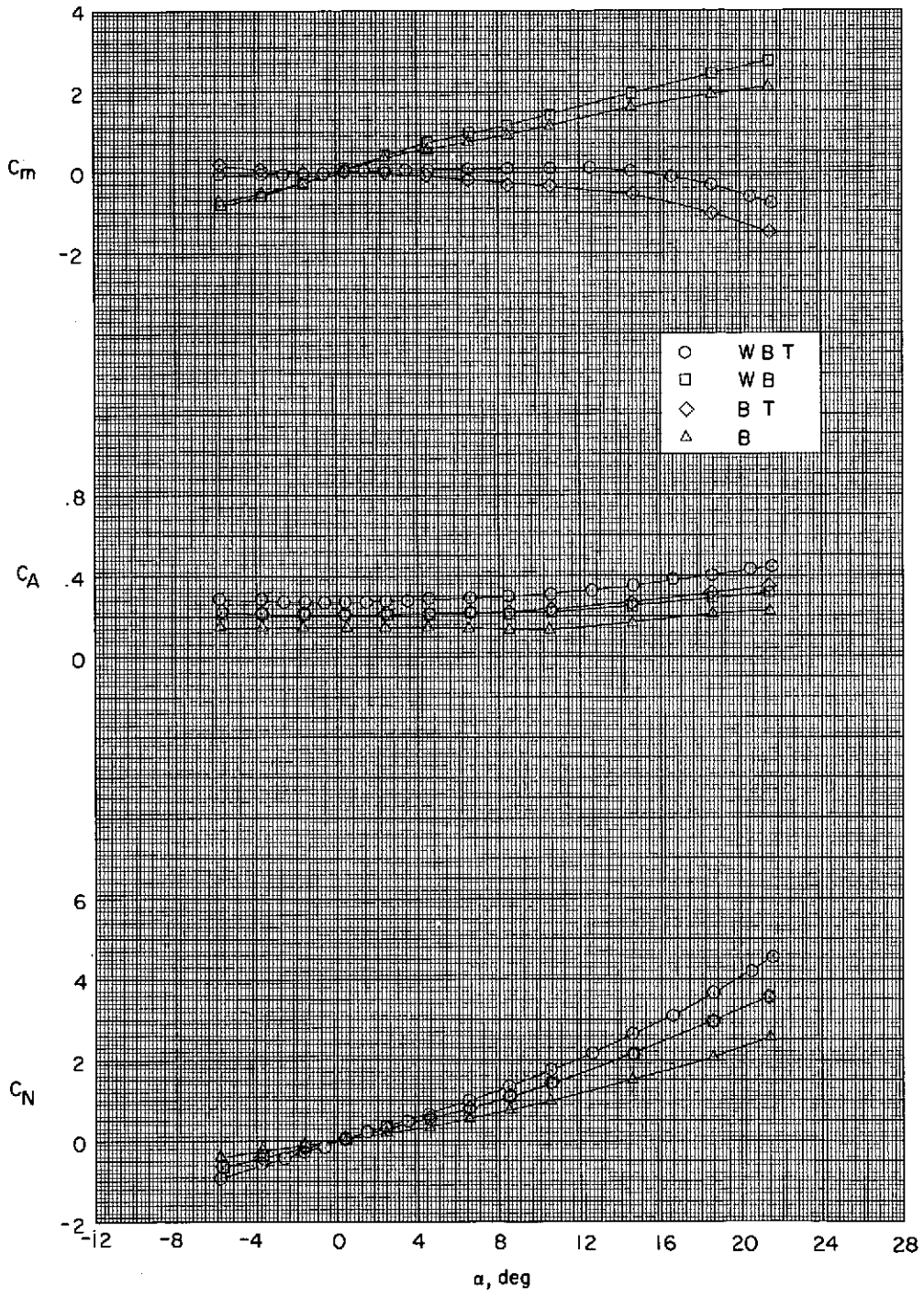

(b) M = 4.63.

Figure 5.- Continued.

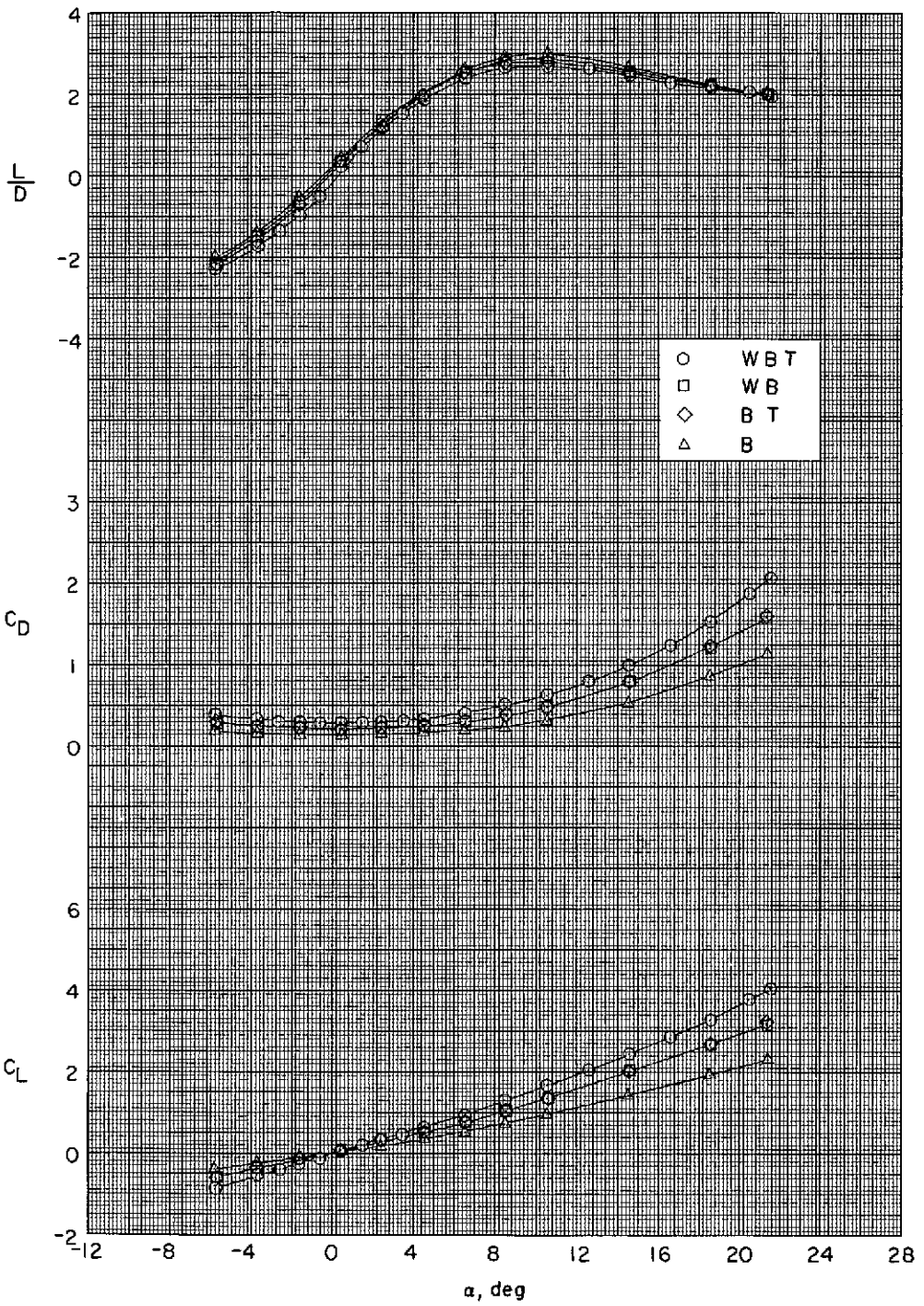

(b) Concluded.

Figure 5.- Concluded.

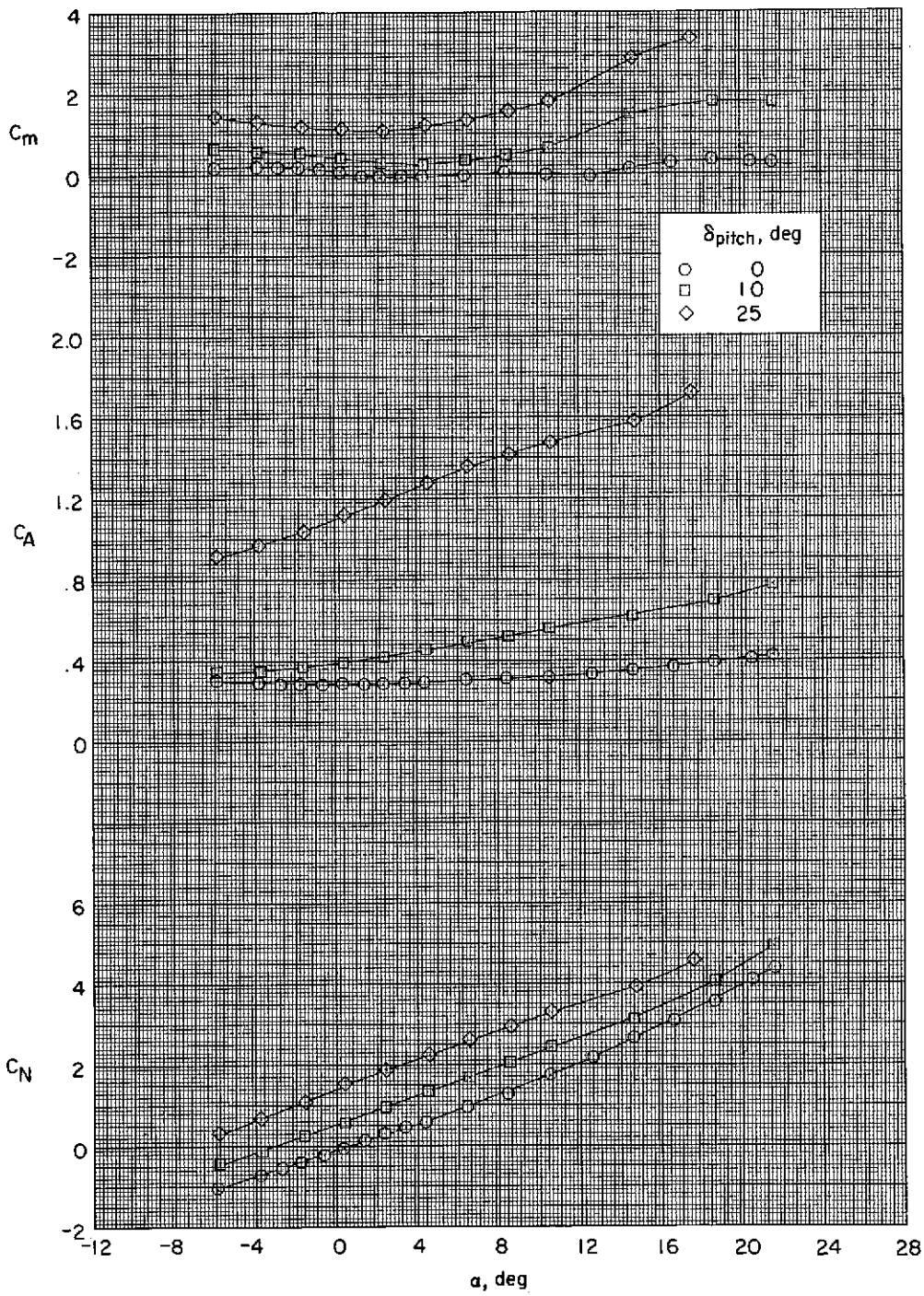

(a) M = 3.95.

Figure 6.- Pitch-control characteristics; $\Phi = 45^0$.

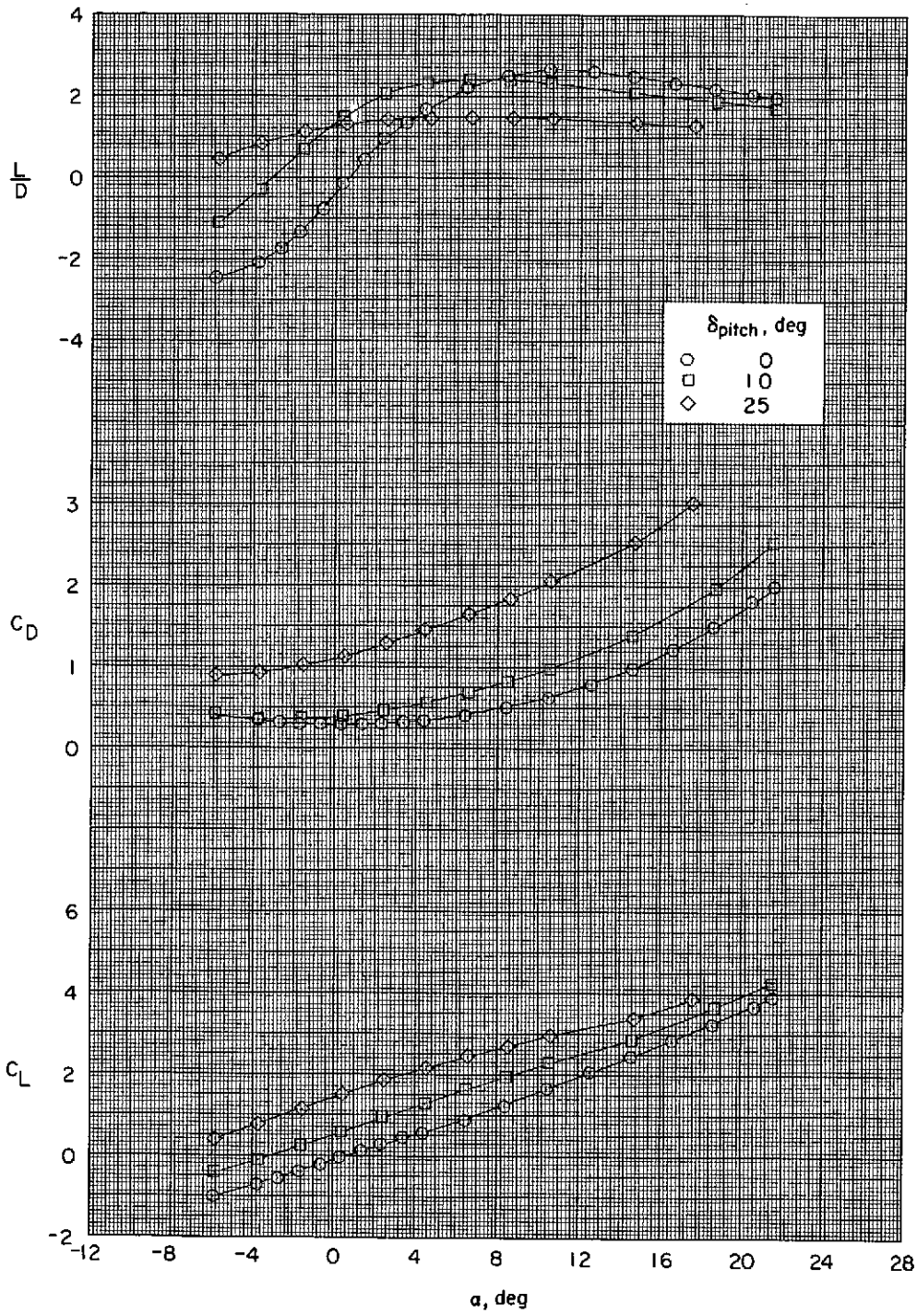

(a) Concluded.

Figure 6.- Continued.

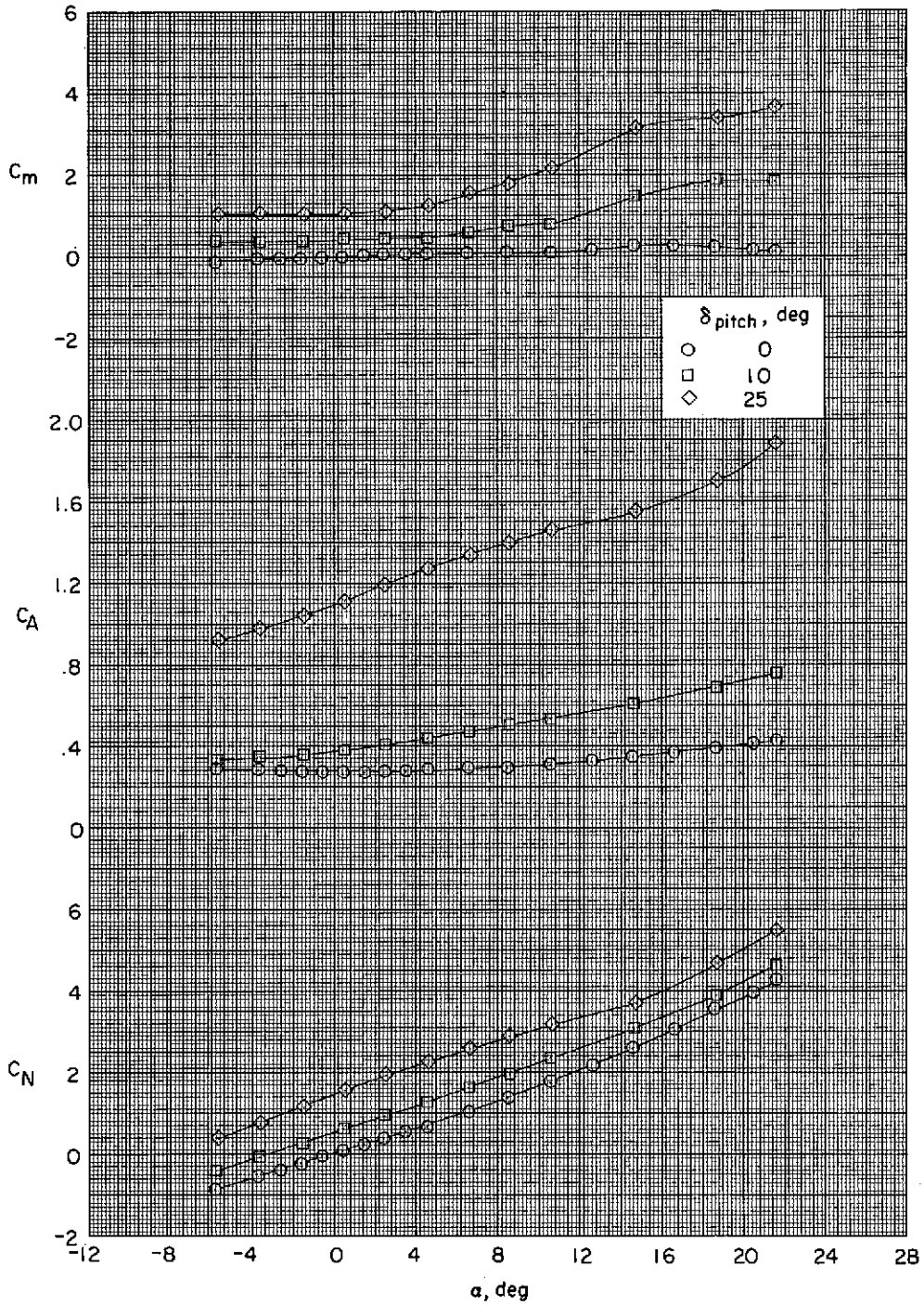

(b) M = 4.63.

Figure 6.- Continued.

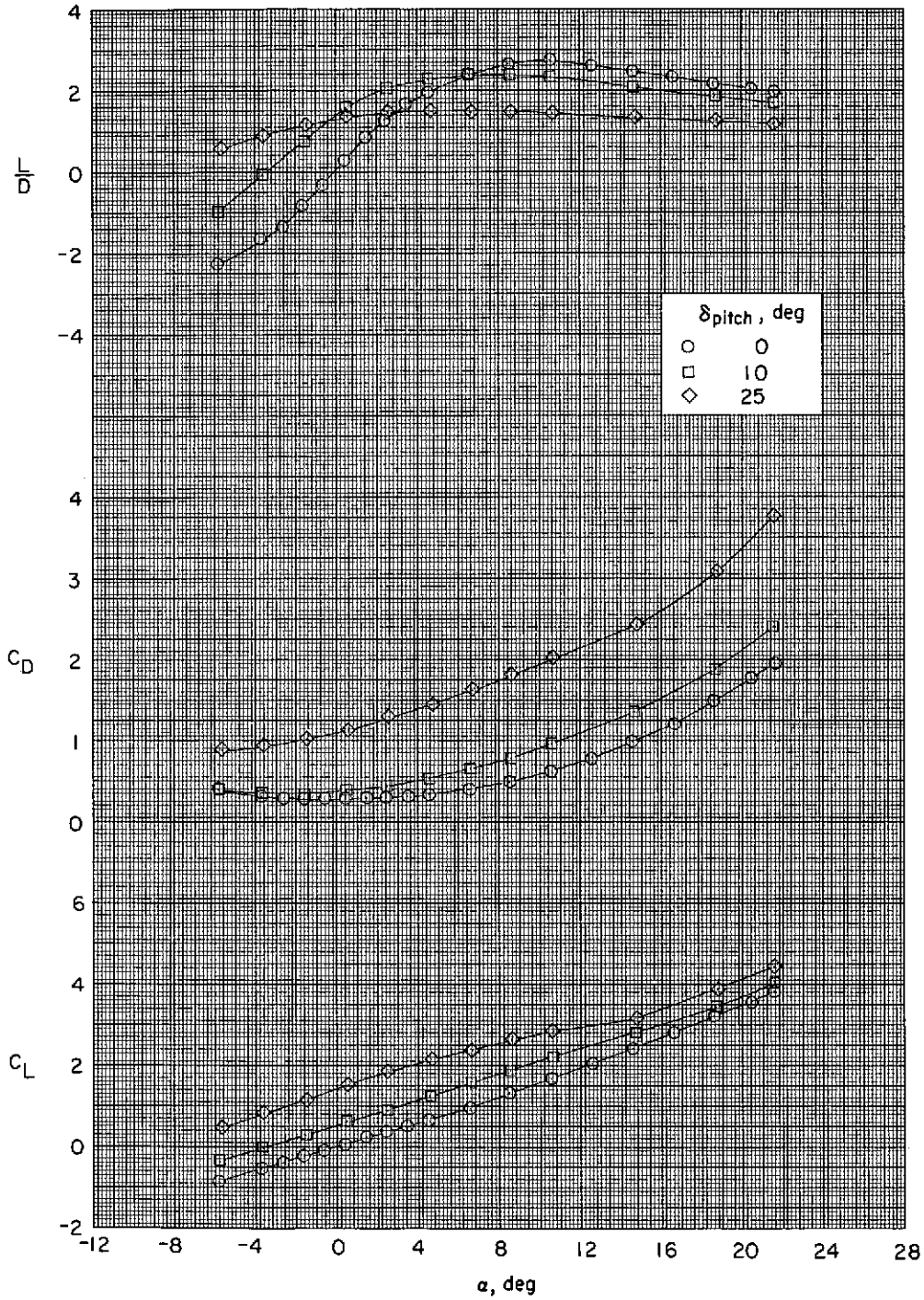

(b) Concluded.

Figure 6.- Concluded.

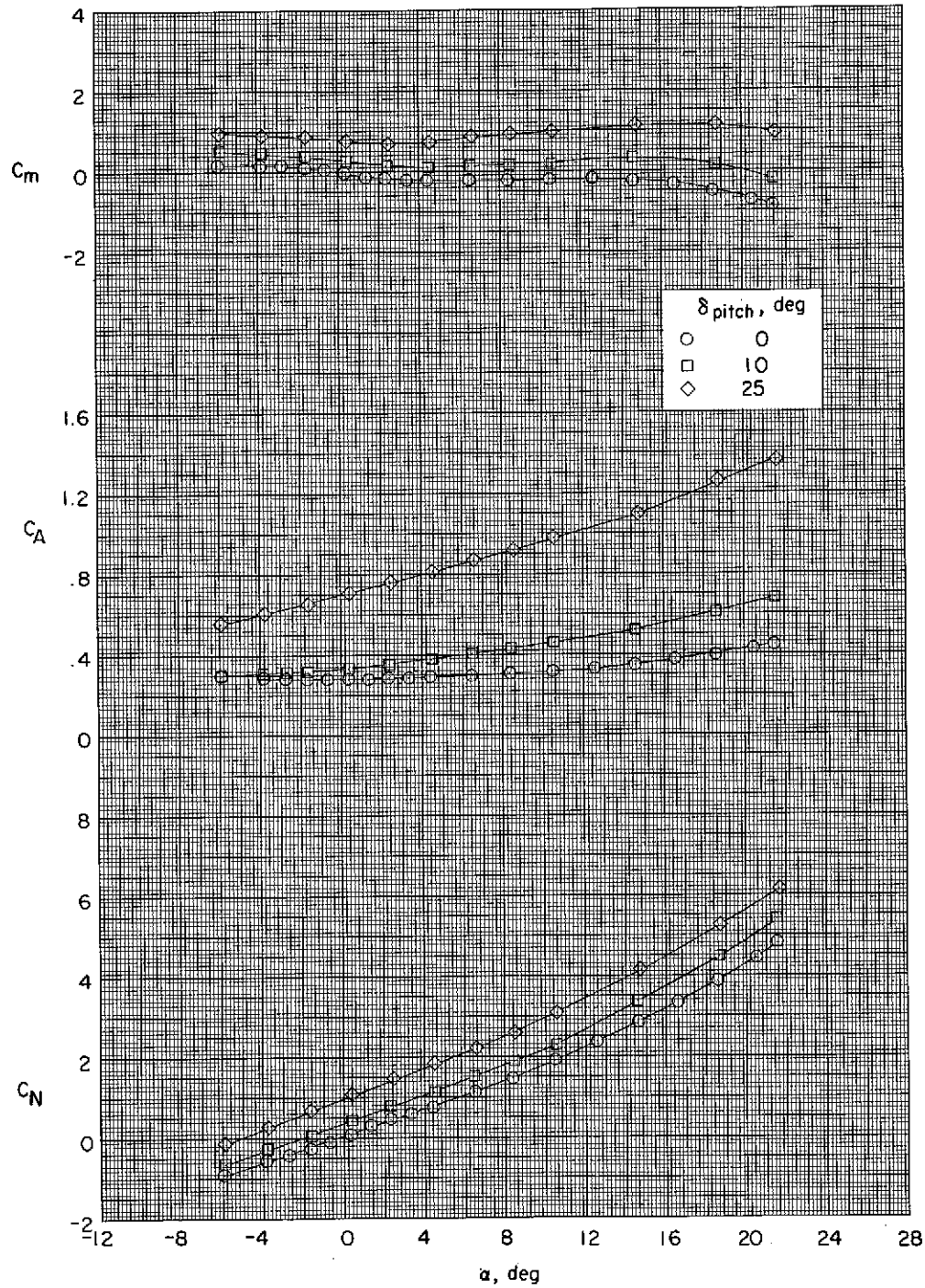

(a) M = 3.95.

Figure 7.- Pitch-control characteristics; $\Phi = 0^0$.

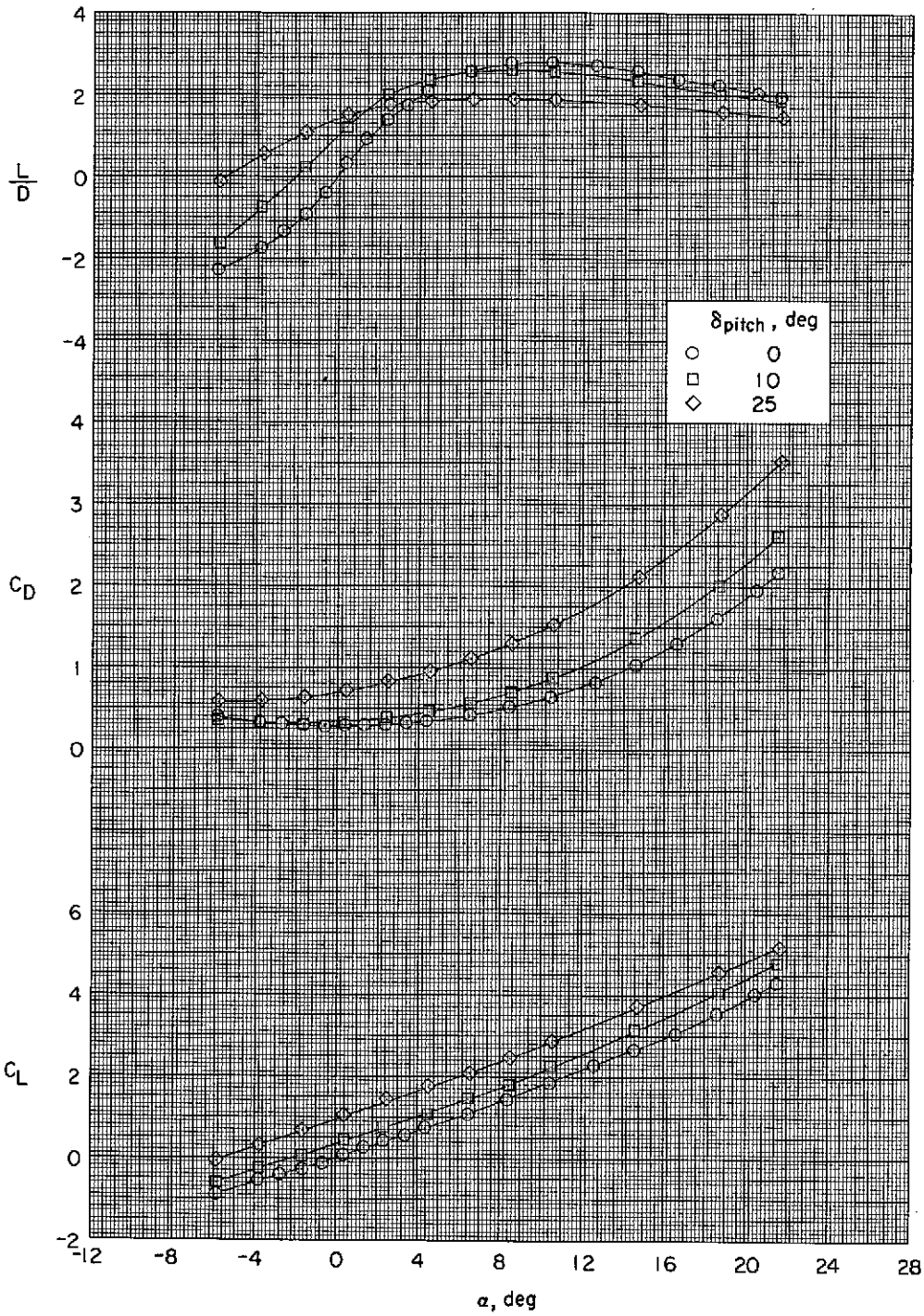

(a) Concluded.

Figure 7.- Continued.

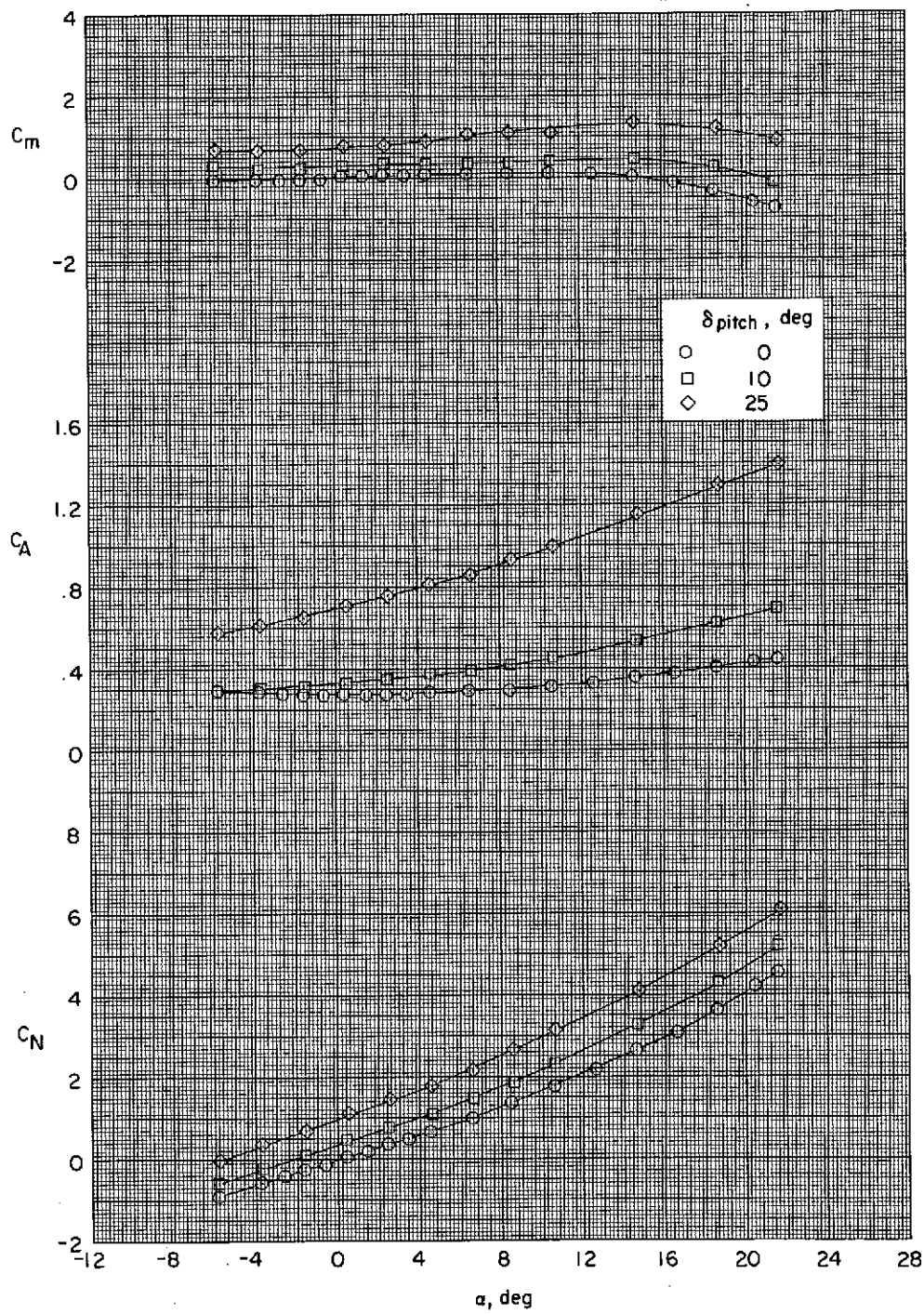

(b) M = 4.63.

Figure 7.- Continued.

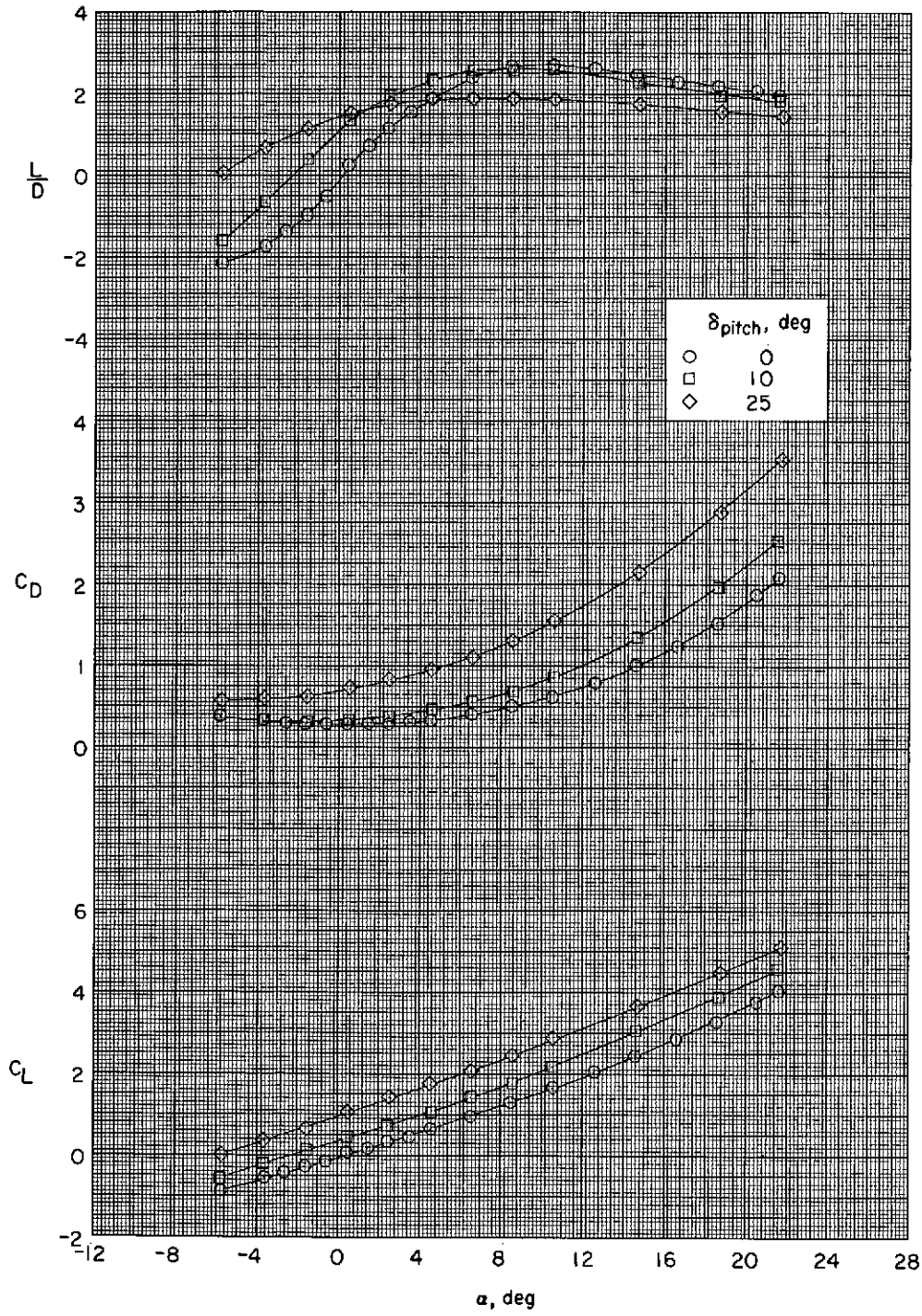

(b) Concluded.

Figure 7.- Concluded.

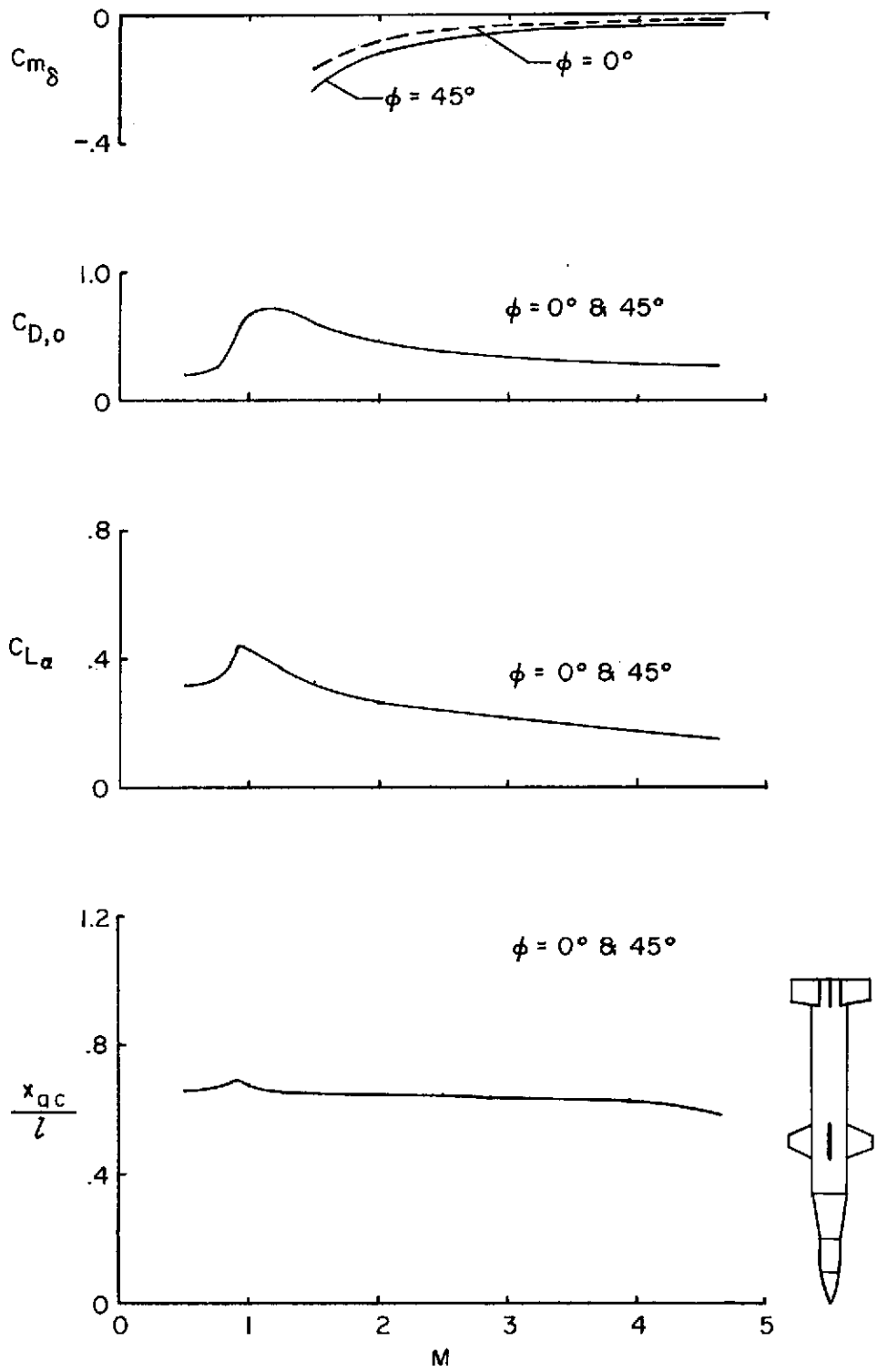

Figure 8.- Variation of longitudinal parameters with Mach number near $\alpha = 0^0$.

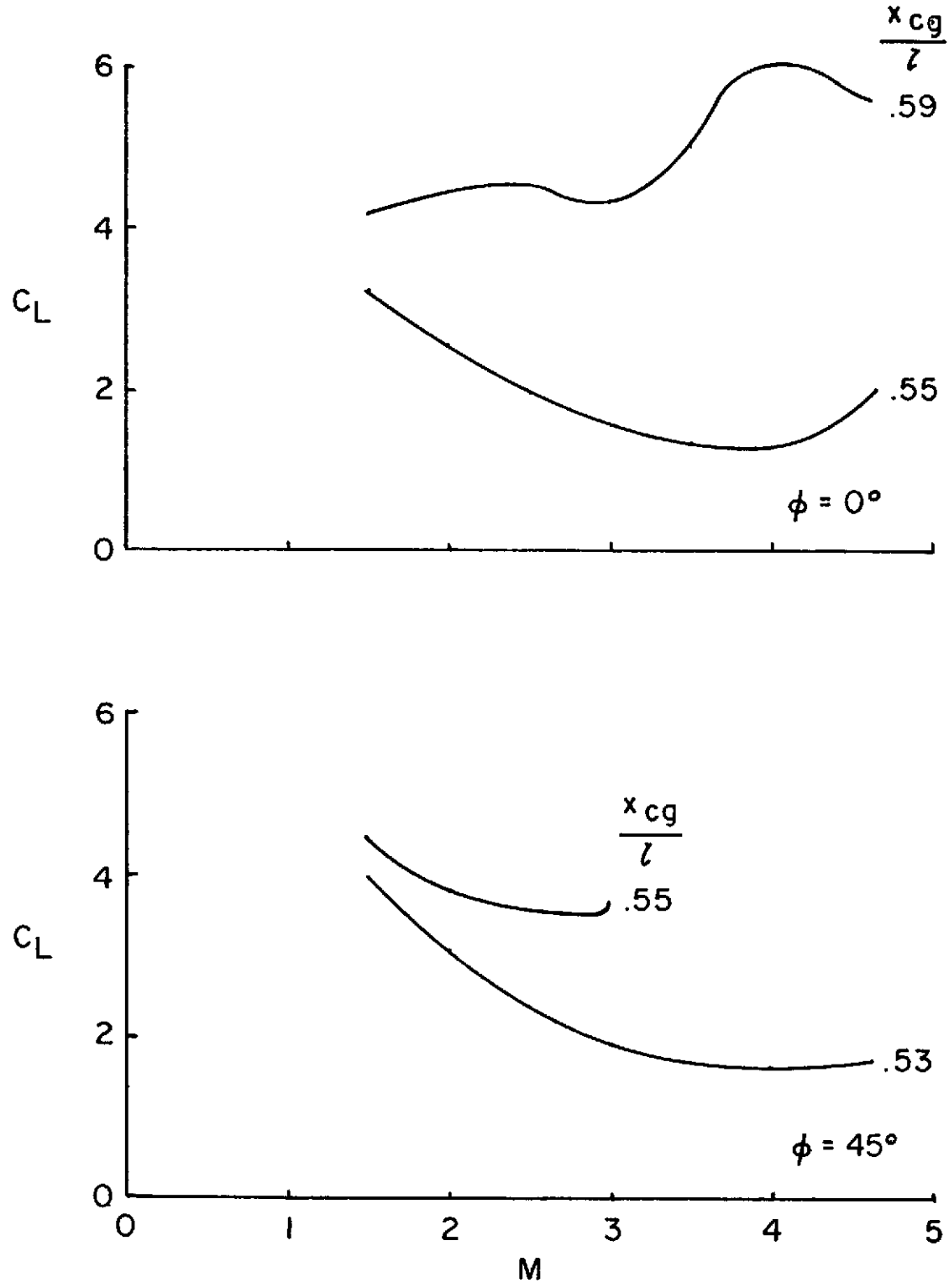

Figure 9.- Variation of trimmed lift coefficient with maximum pitch-control deflection of 25^0.

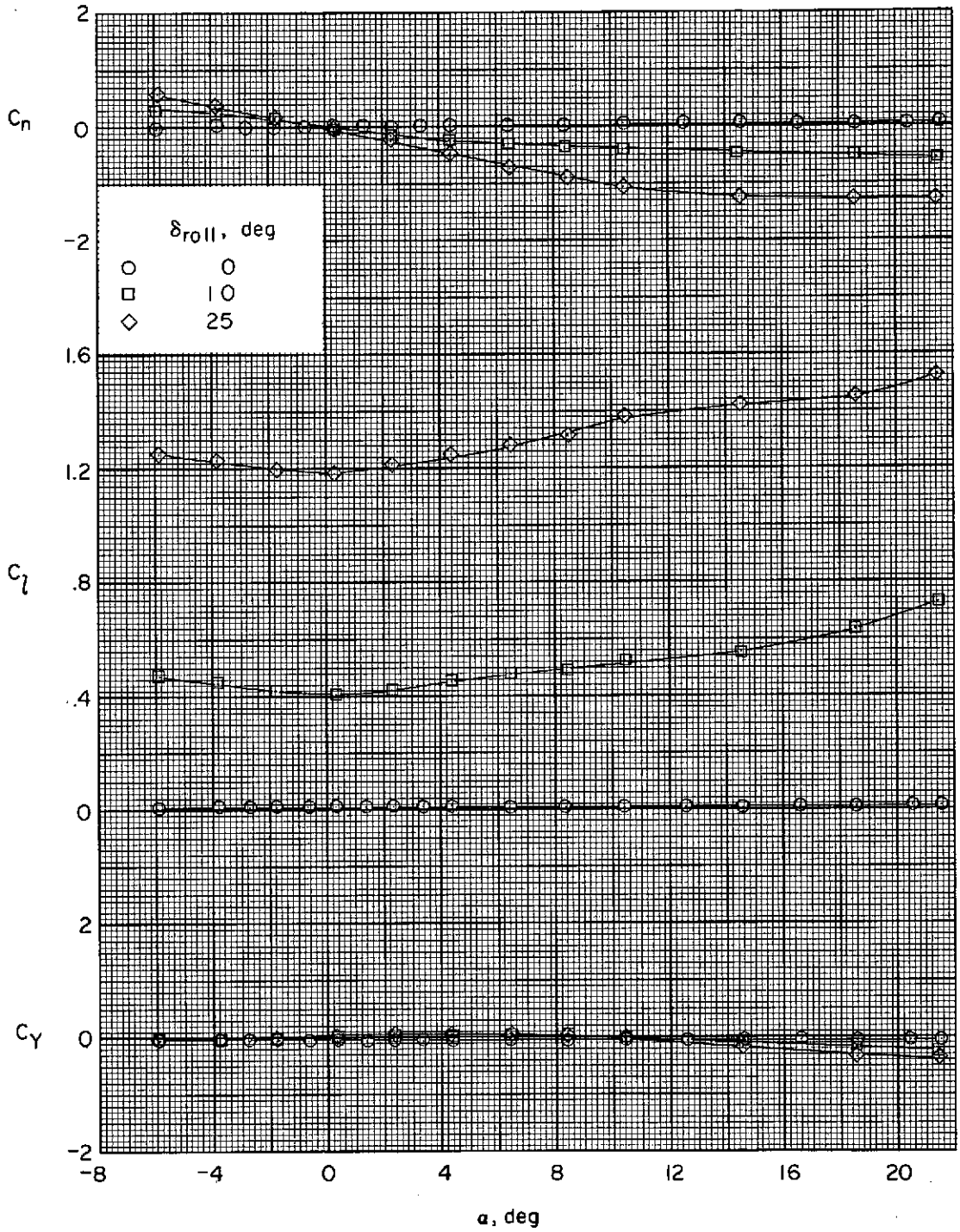

(a) M = 3.95.

Figure 10.- Roll-control characteristics; $\Phi = 45^{0}$; four wings deflected.

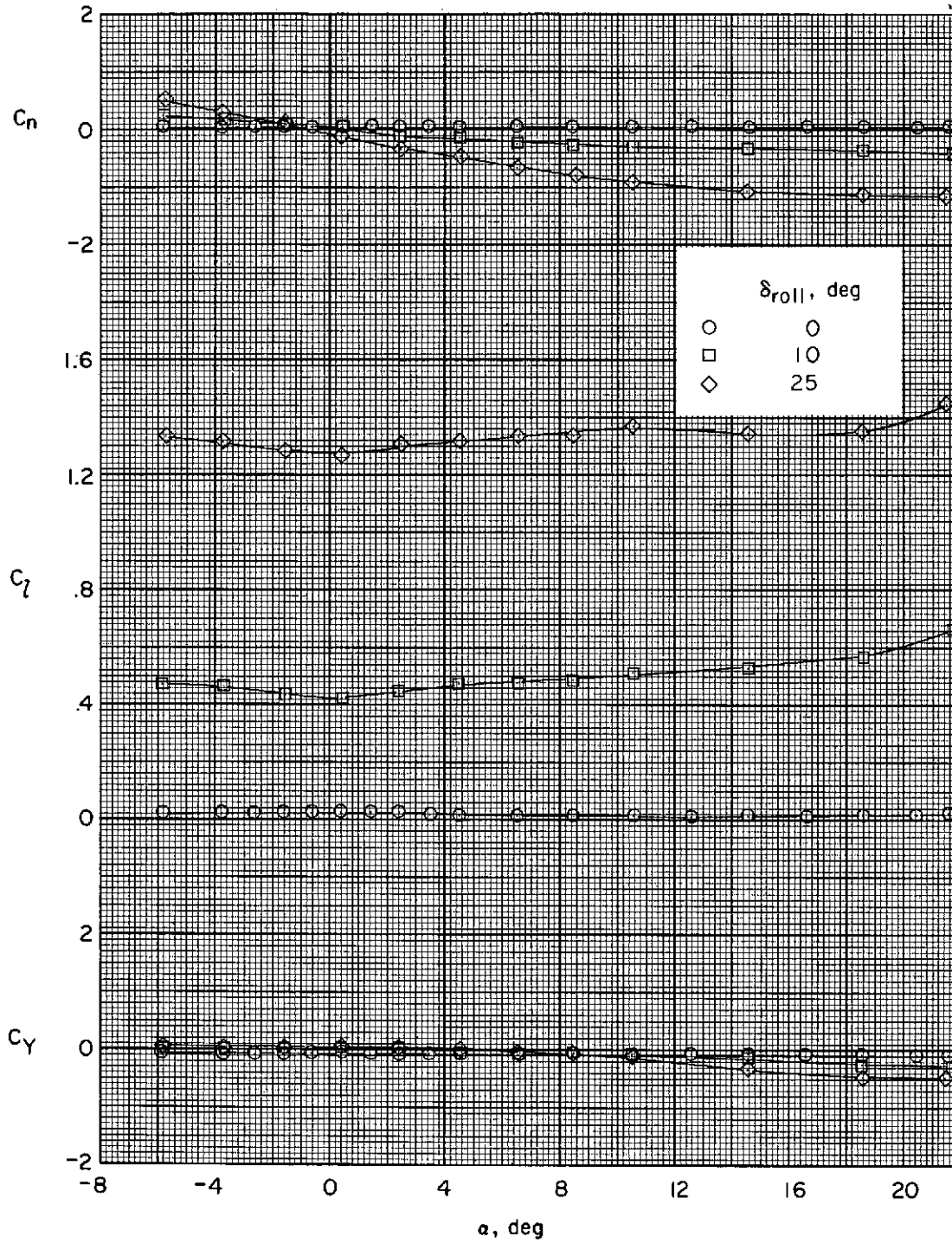

(b) M = 4.63.

Figure 10.- Concluded.

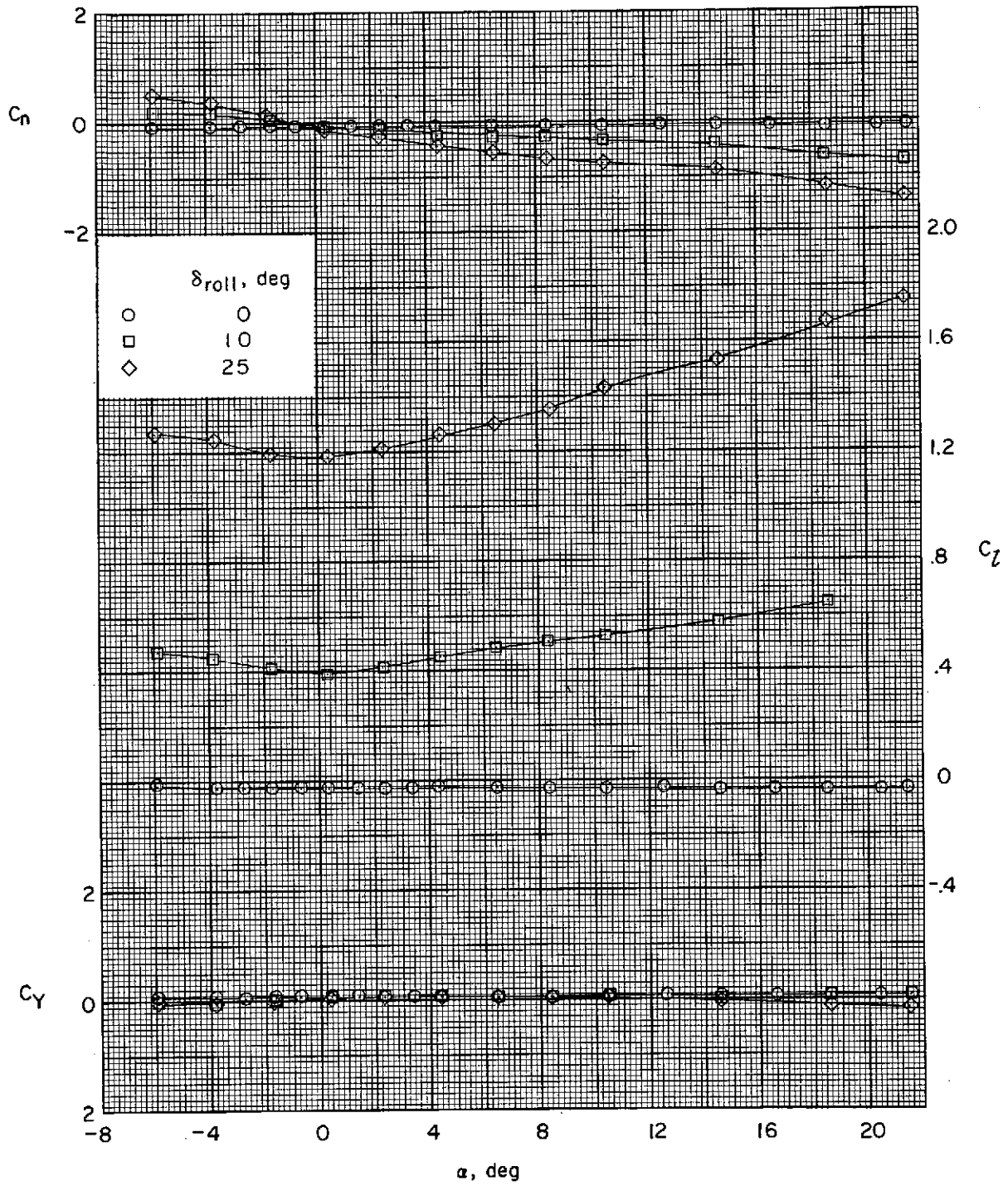

(a) M = 3.95.

Figure 11.- Roll-control characteristics; $\Phi = 0^0$; four wings deflected.

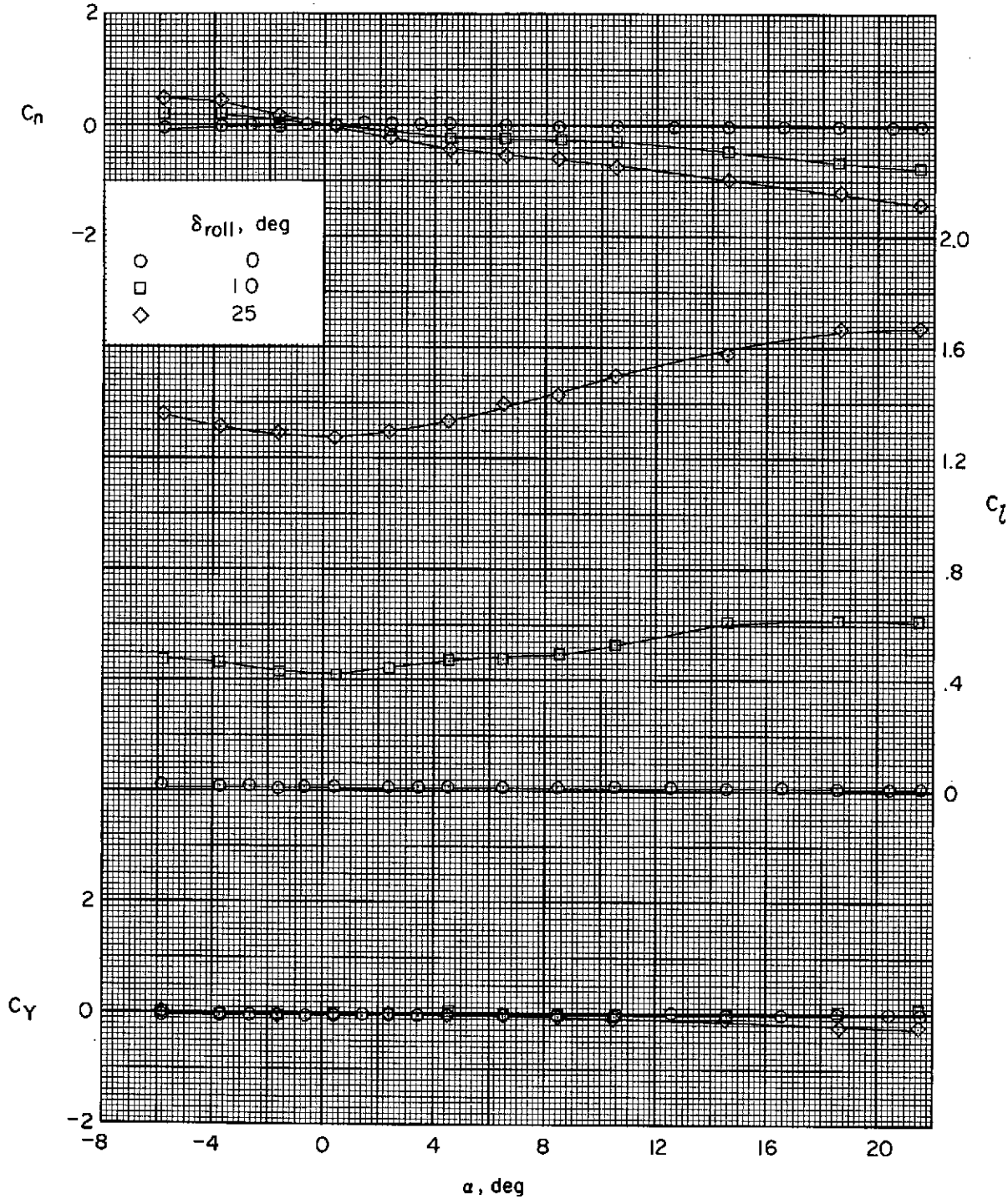

(b) M = 4.63.

Figure 11.- Concluded.

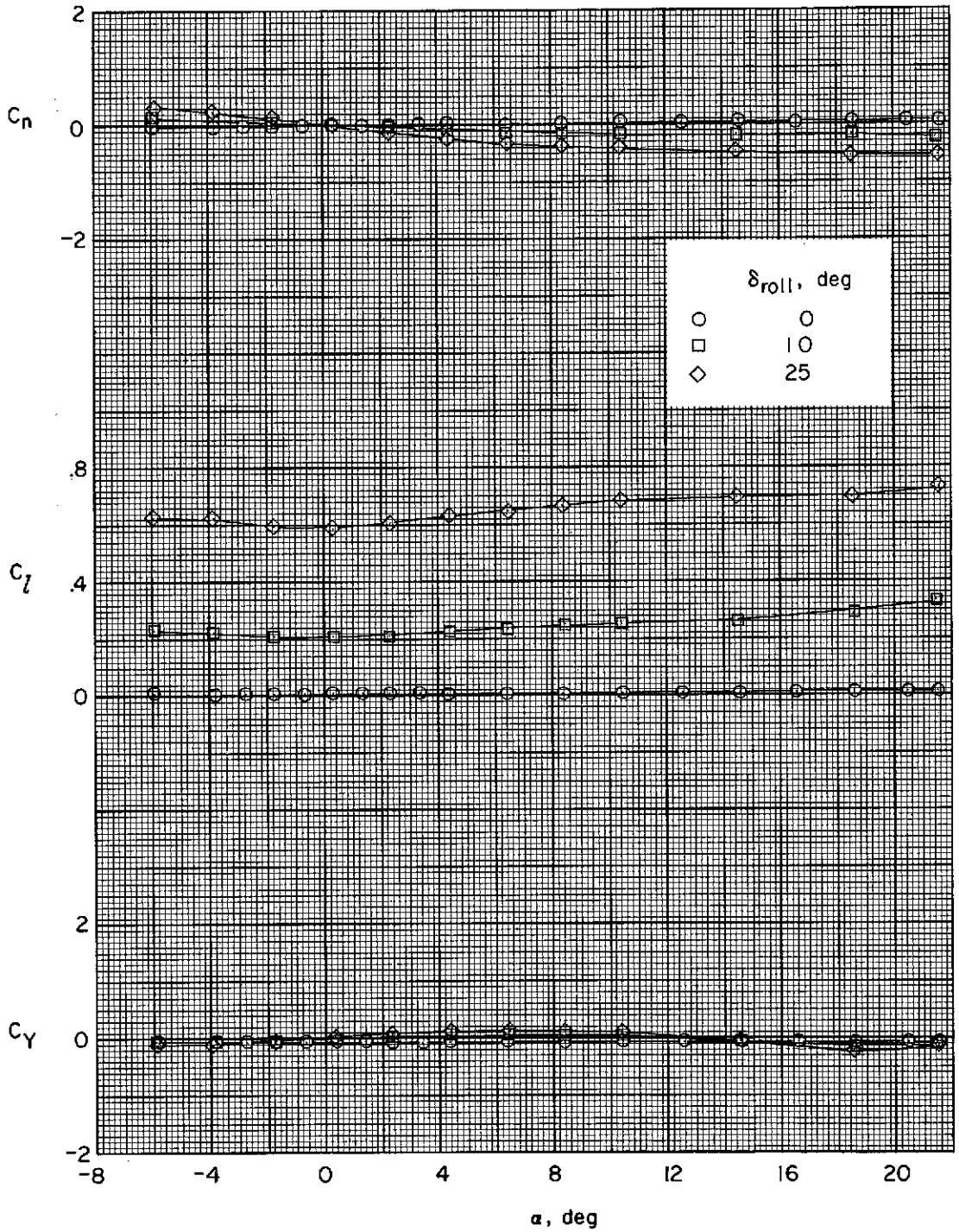

(a) M = 3.95.

Figure 12.- Roll-control characteristics; $\Phi = 45^0$; two wings deflected.

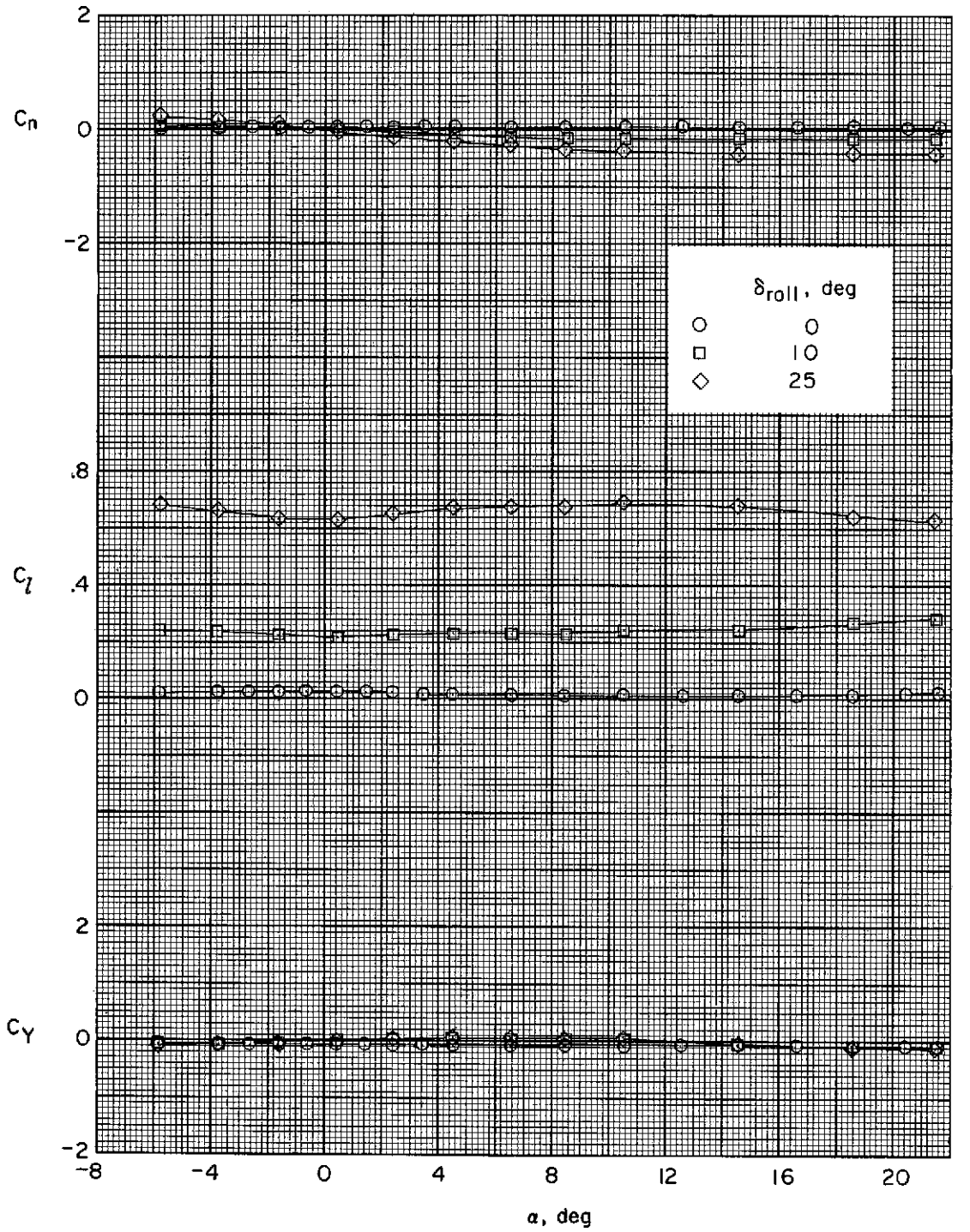

(b) M = 4.63.

Figure 12.- Concluded.

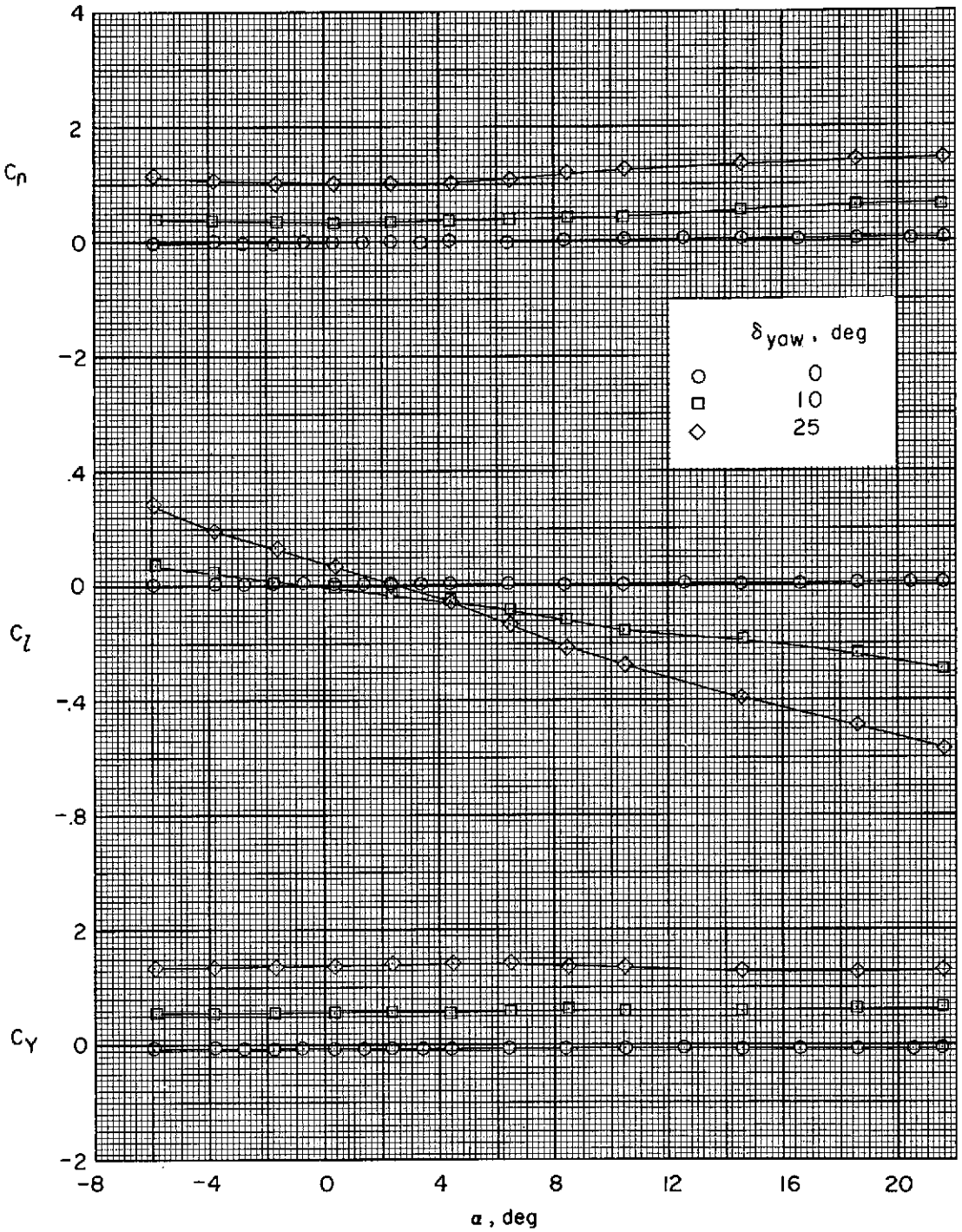

(a) M = 3.95.

Figure 13.- Yaw-control deflection; $\Phi = 45^{0}$; four wings deflected.

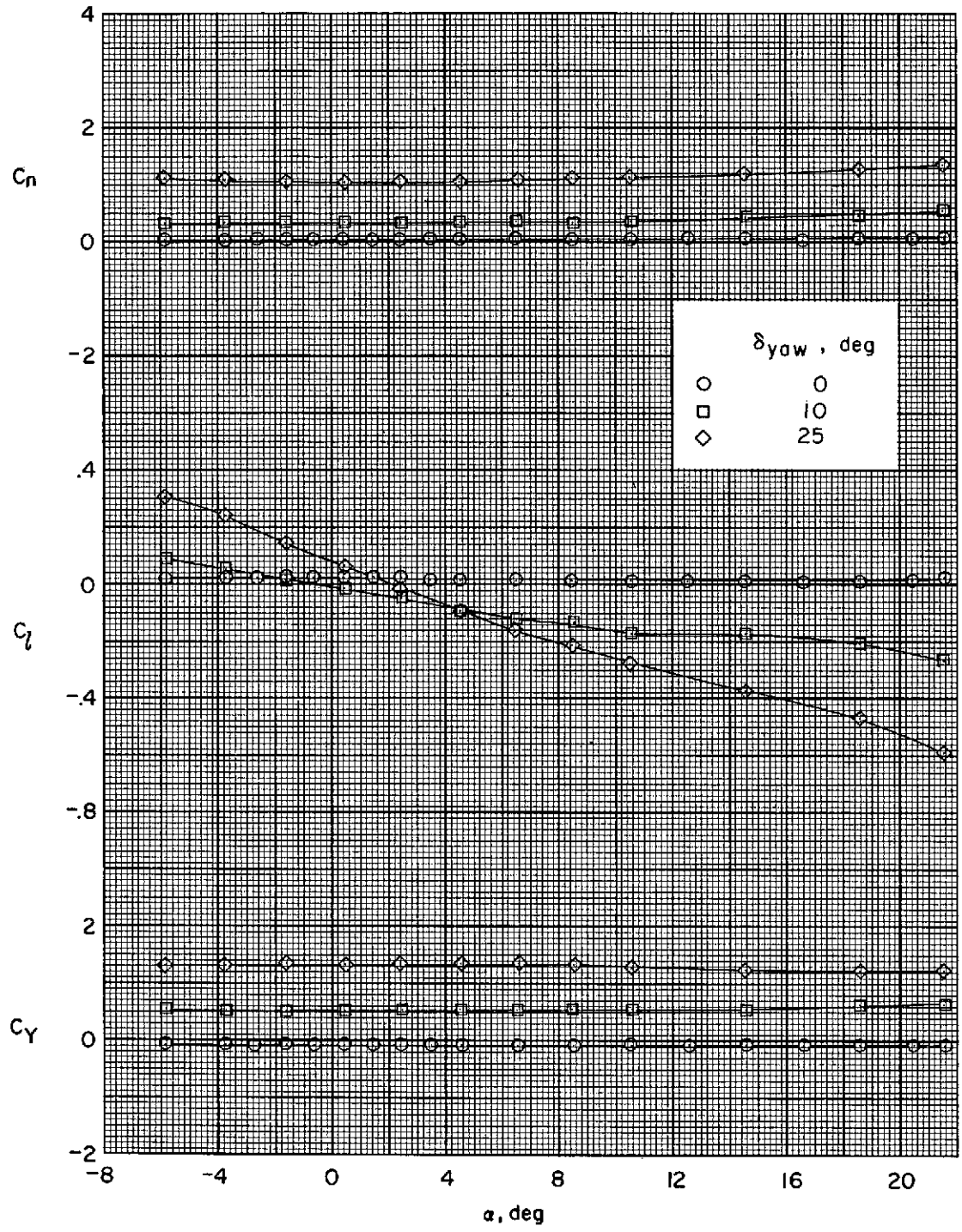

(b) M = 4.63.

Figure 13.- Concluded.

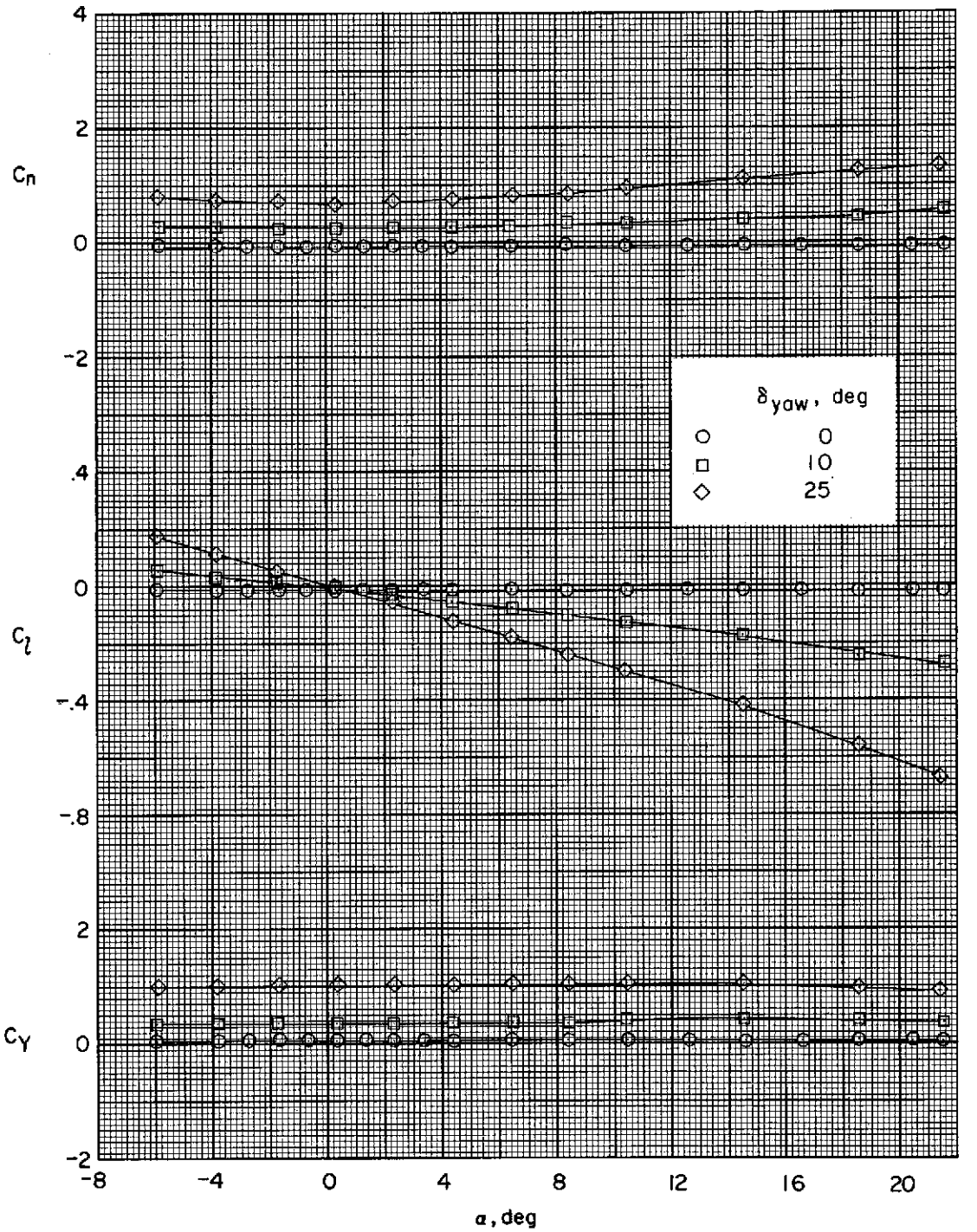

(a) M = 3.95.

Figure 14.- Yaw control characteristics; $\Phi = 0^0$; two wings deflected.

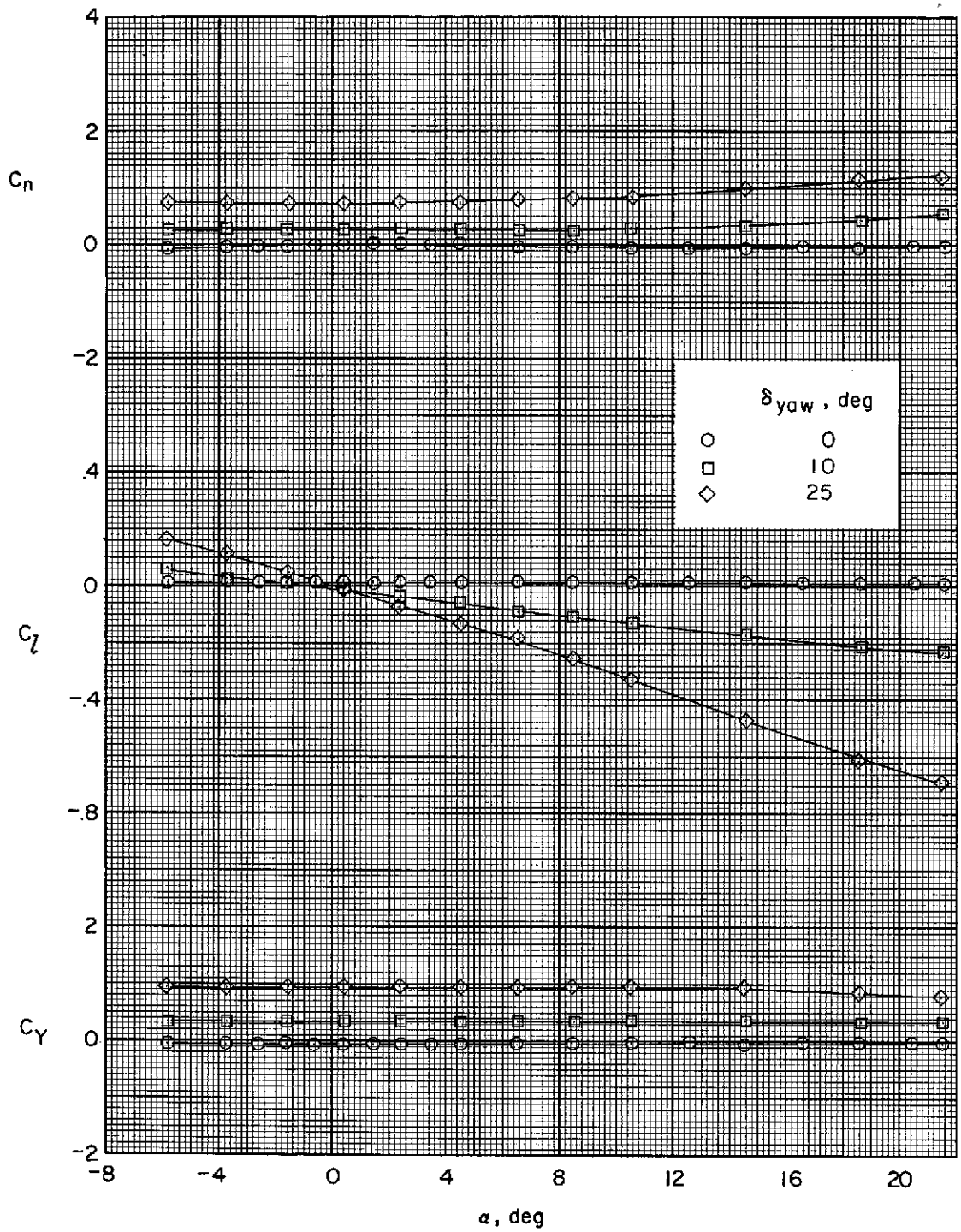

(b) M = 4.63.

Figure 14.- Concluded.

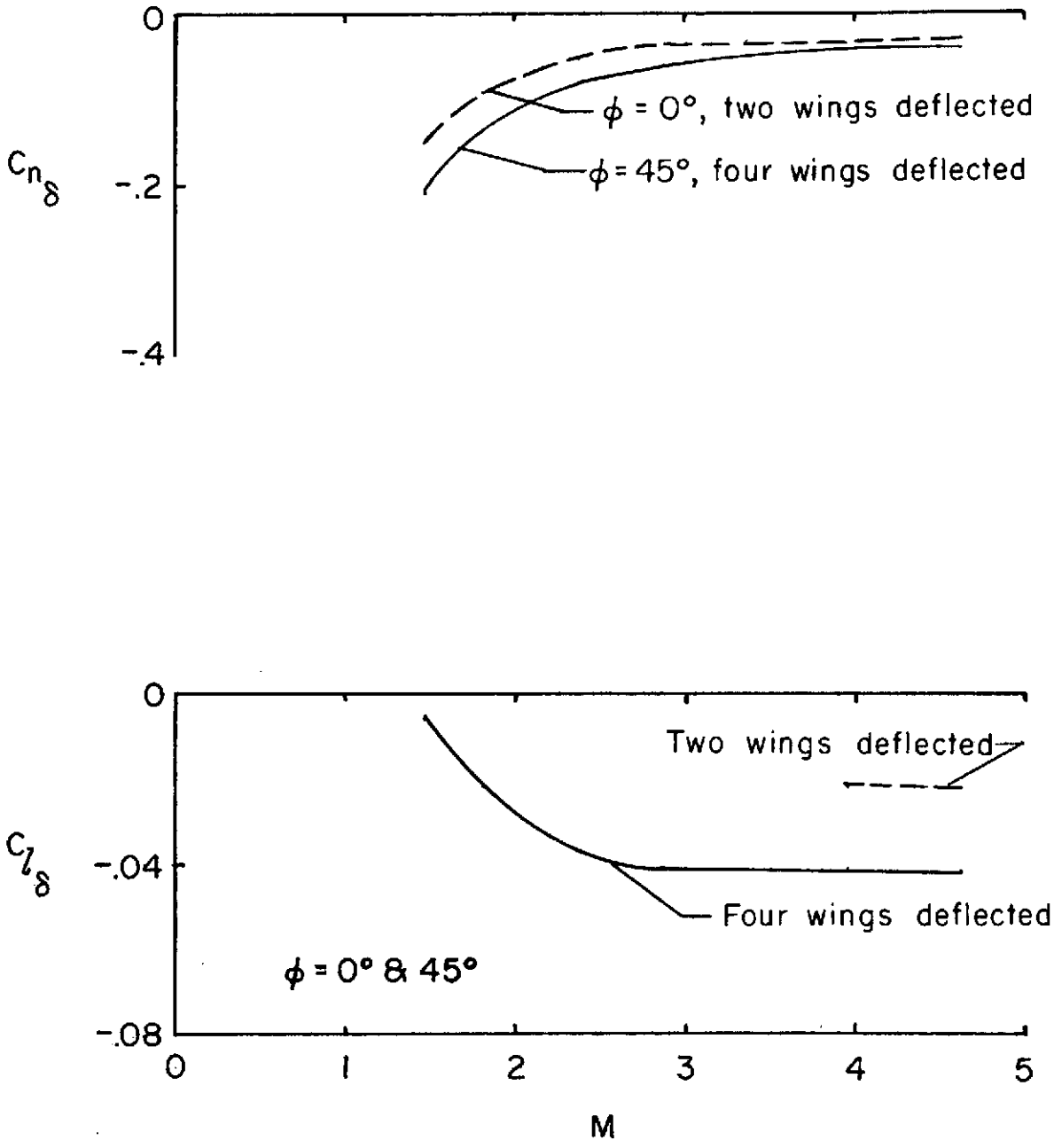

Figure 15.- Variation of lateral-control parameters with Mach number; $\alpha = 0^0$.

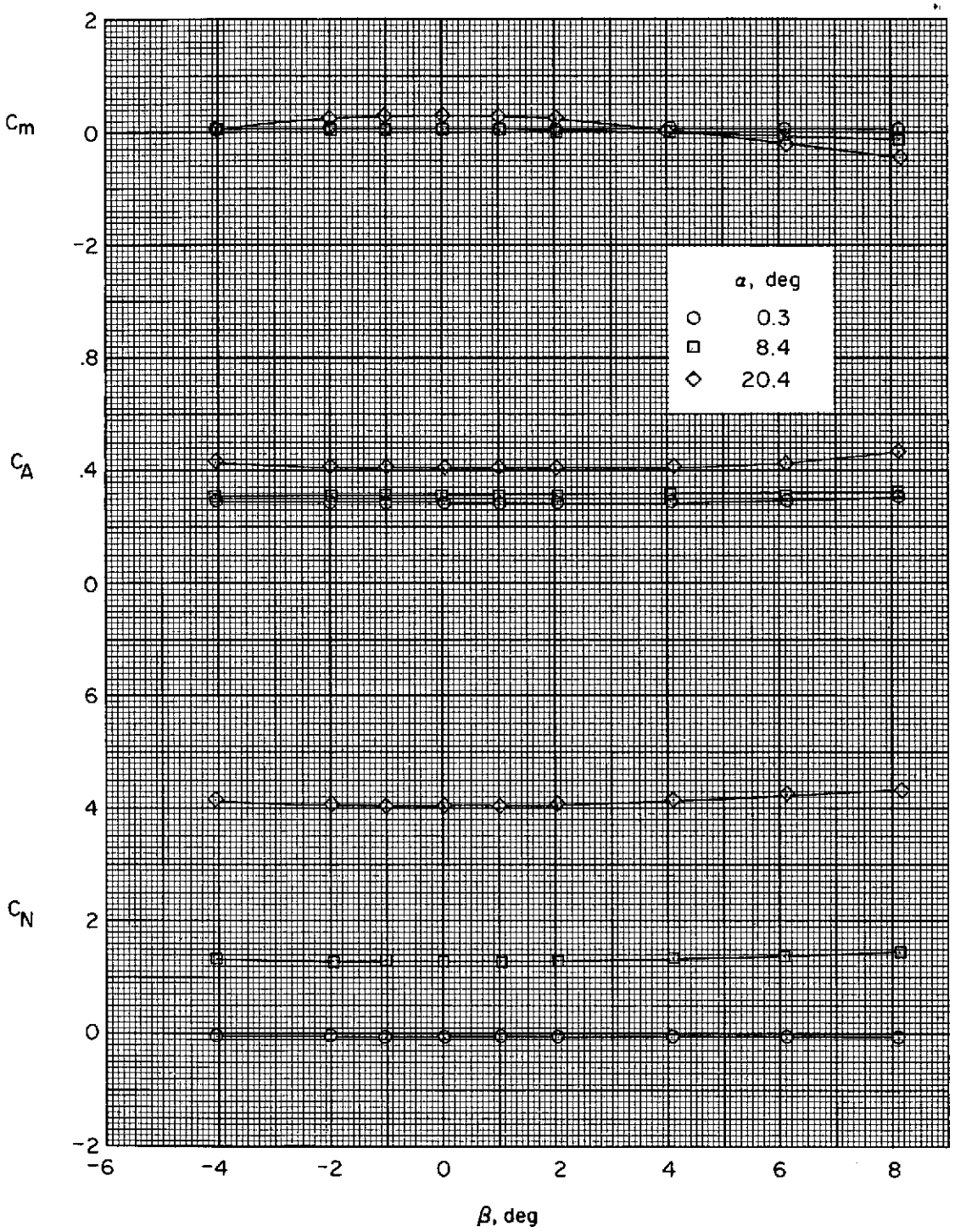

(a) M = 3.95.

Figure 16.- Variation of aerodynamic characteristics with sideslip; zero control deflection; $\Phi = 45^0$.

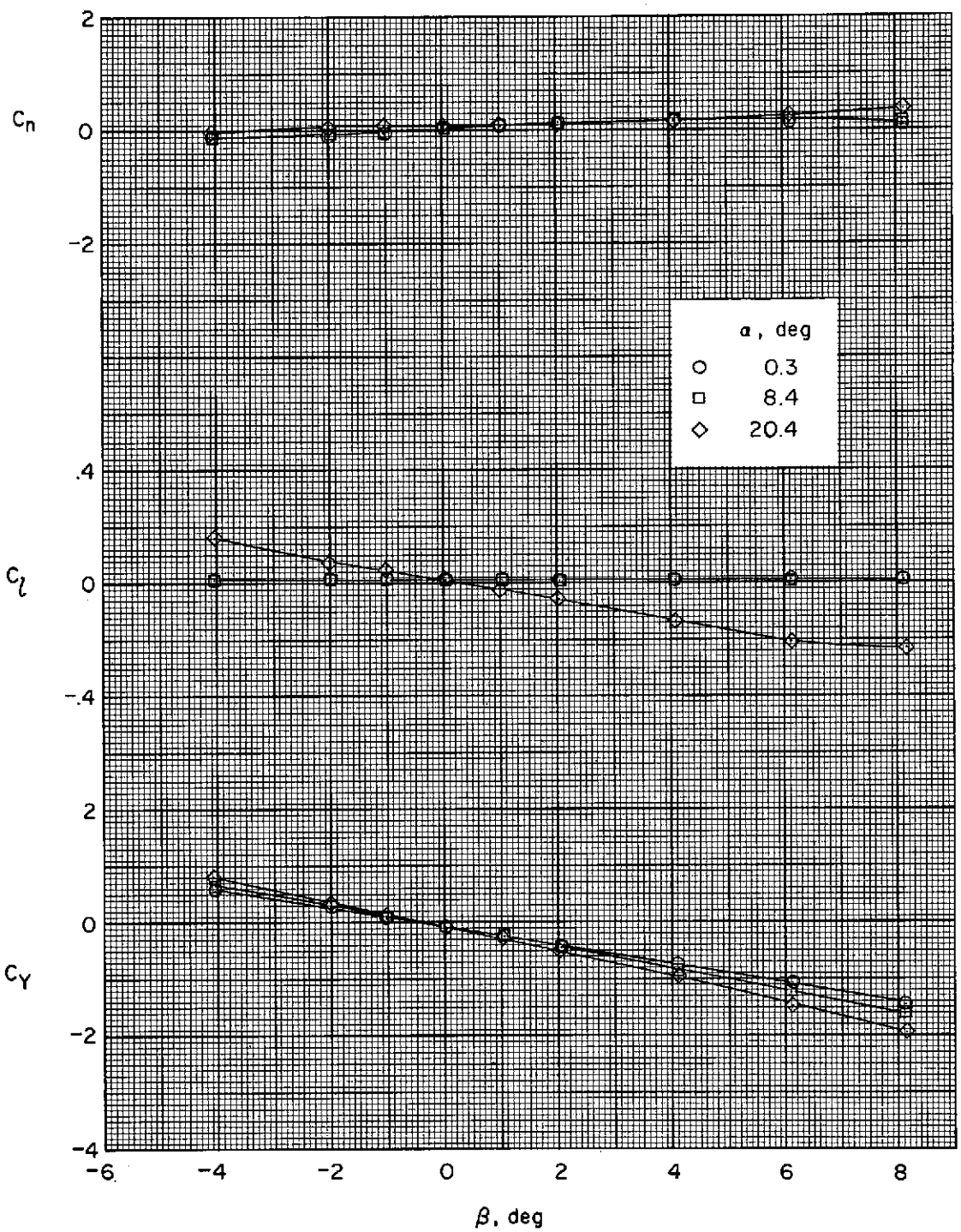

(a) Concluded.

Figure 16.- Continued.

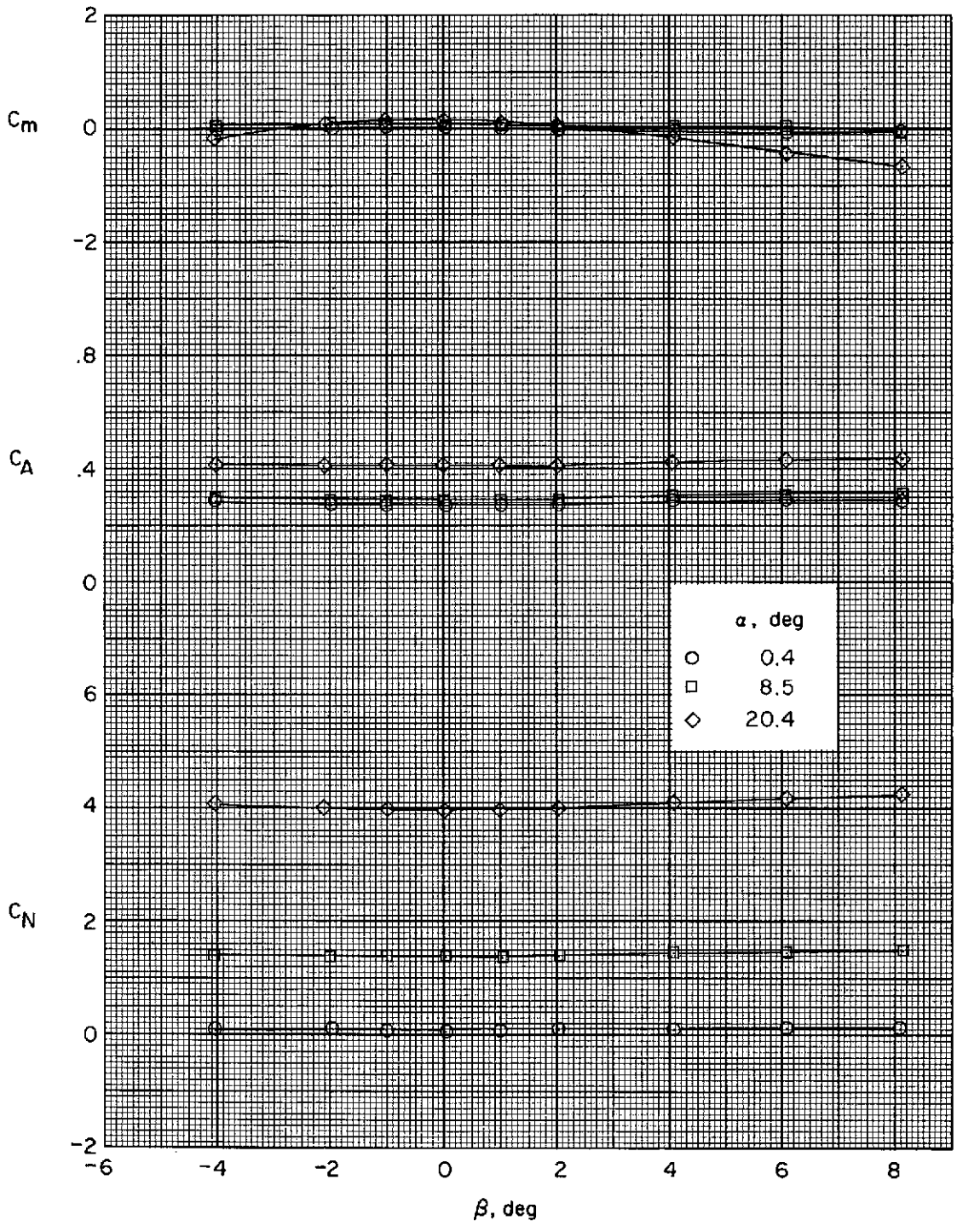

(b) M = 4.63.

Figure 16.- Continued.

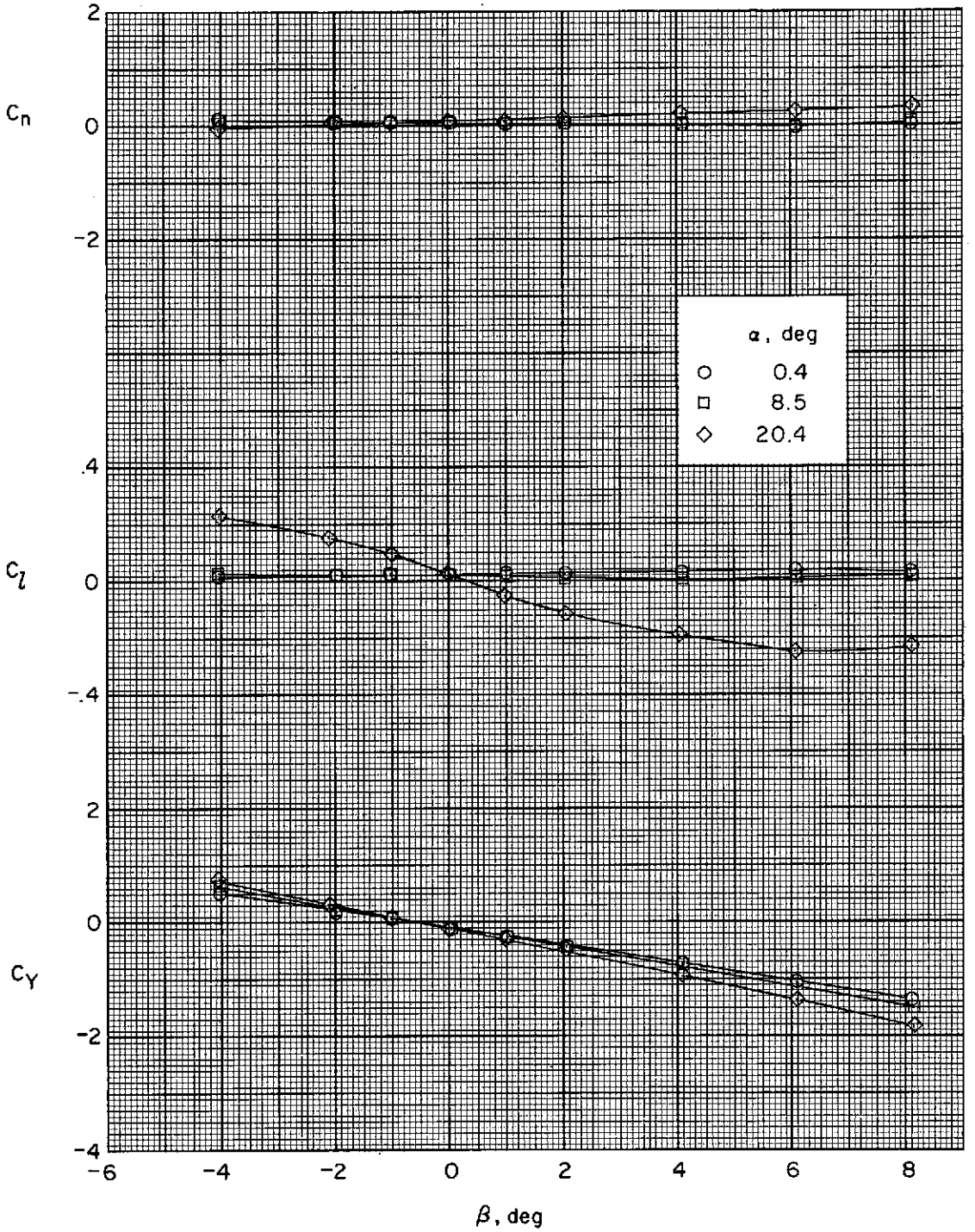

(b) Concluded.

Figure 16.- Concluded.

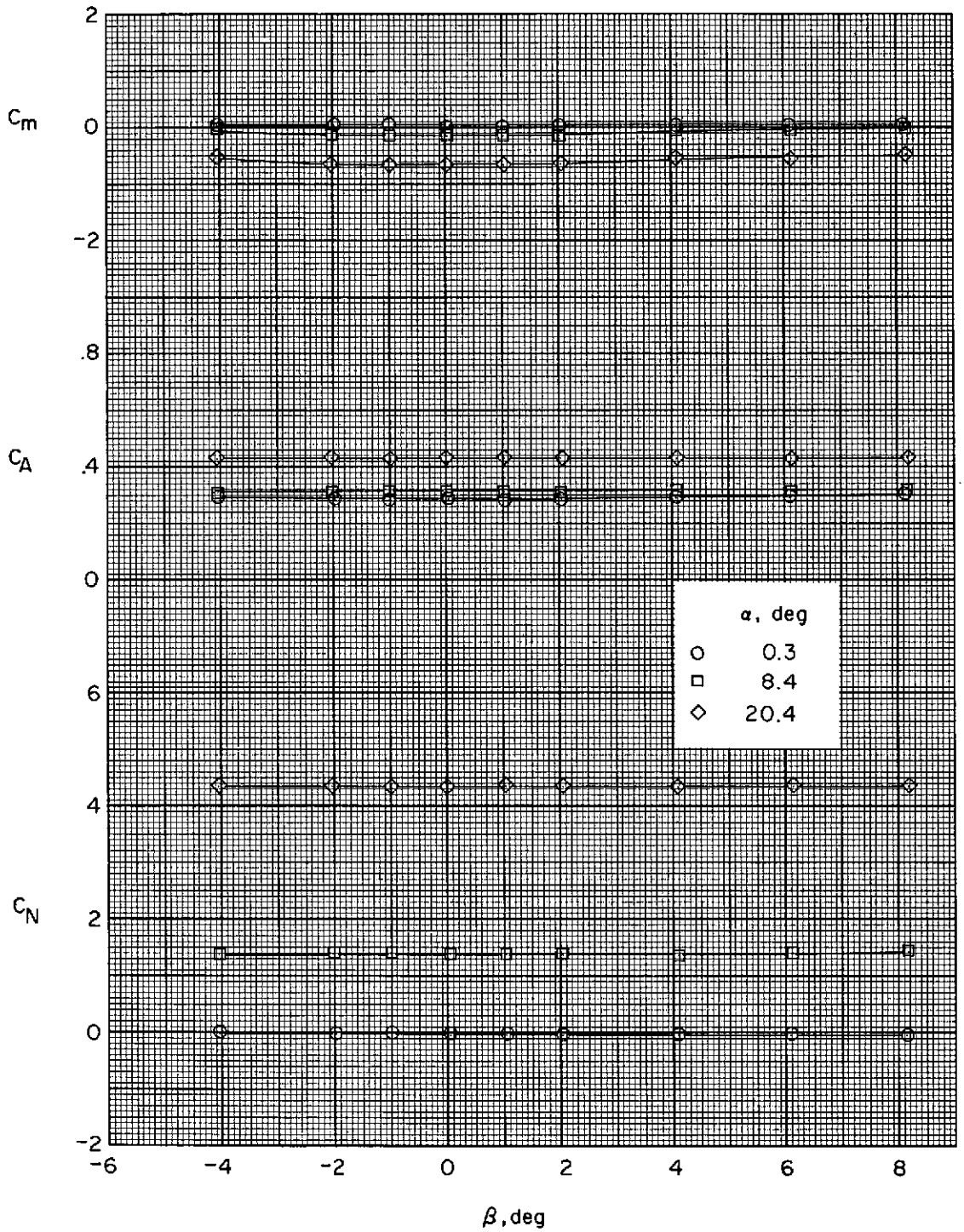

(a) M = 3.95.

Figure 17.- Variation of aerodynamic characteristics with sideslip; zero control deflection; $\Phi = 0^{0}$.

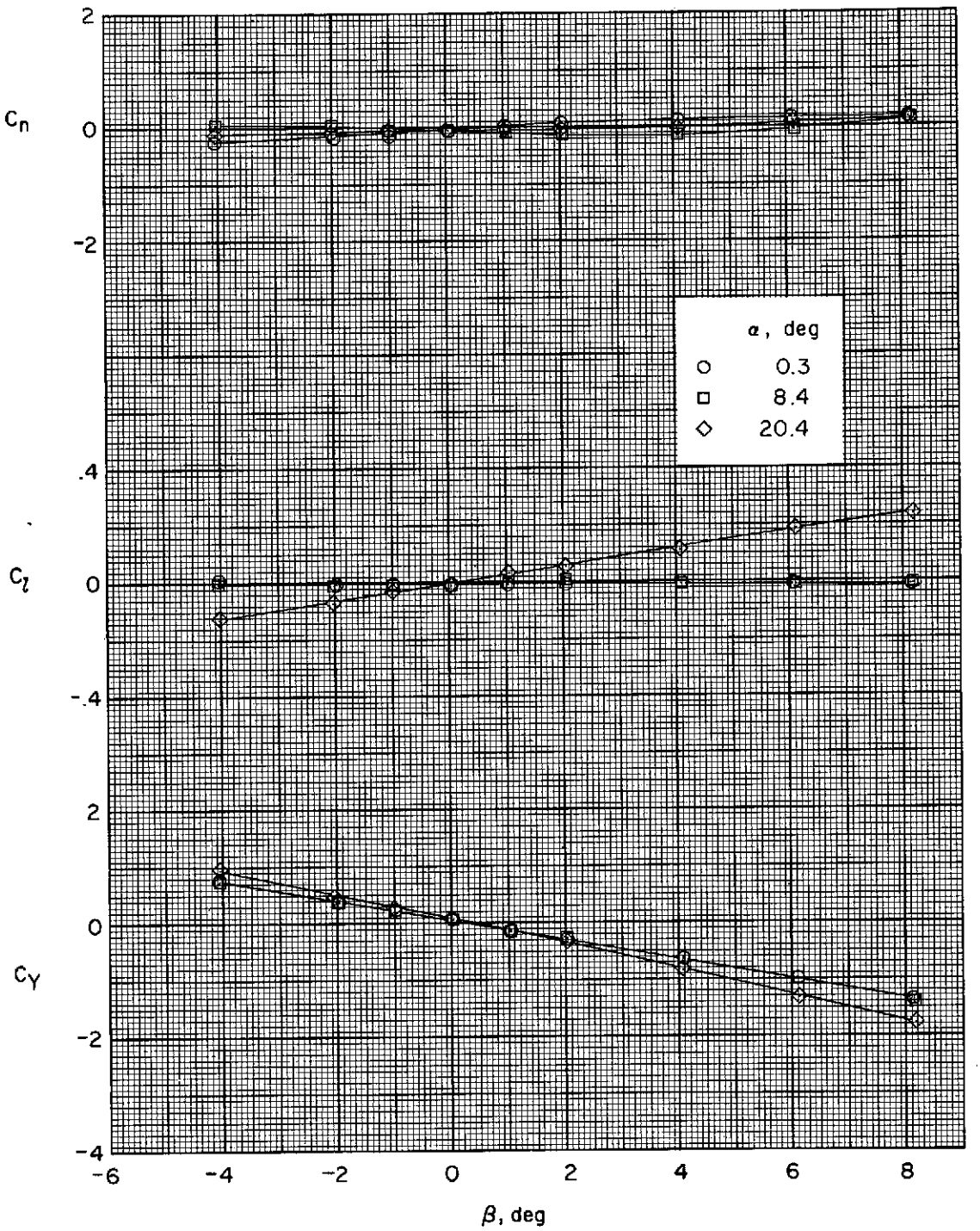

(a) Concluded.

Figure 17.- Continued.

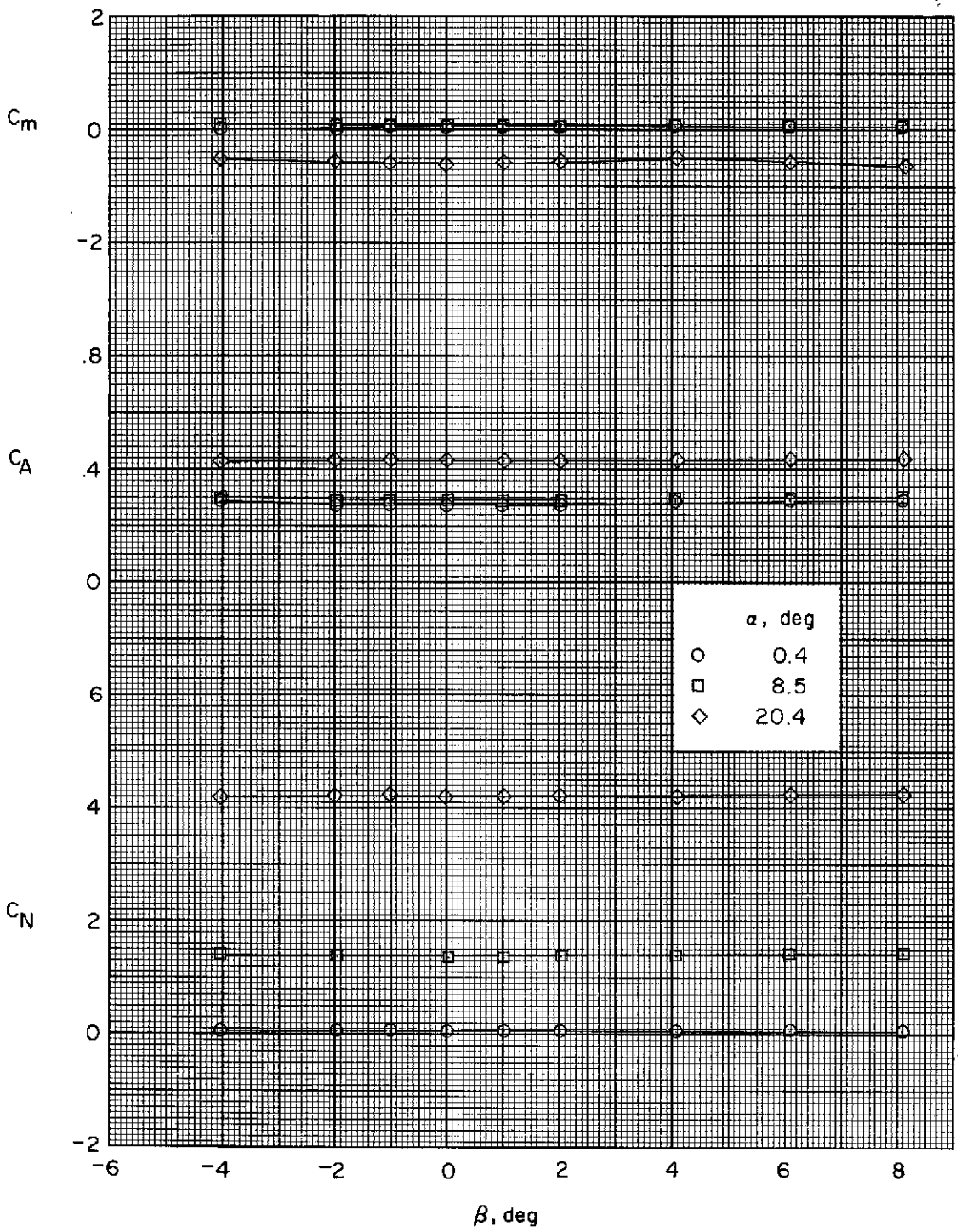

(b) M = 4.63.

Figure 17.- Continued.

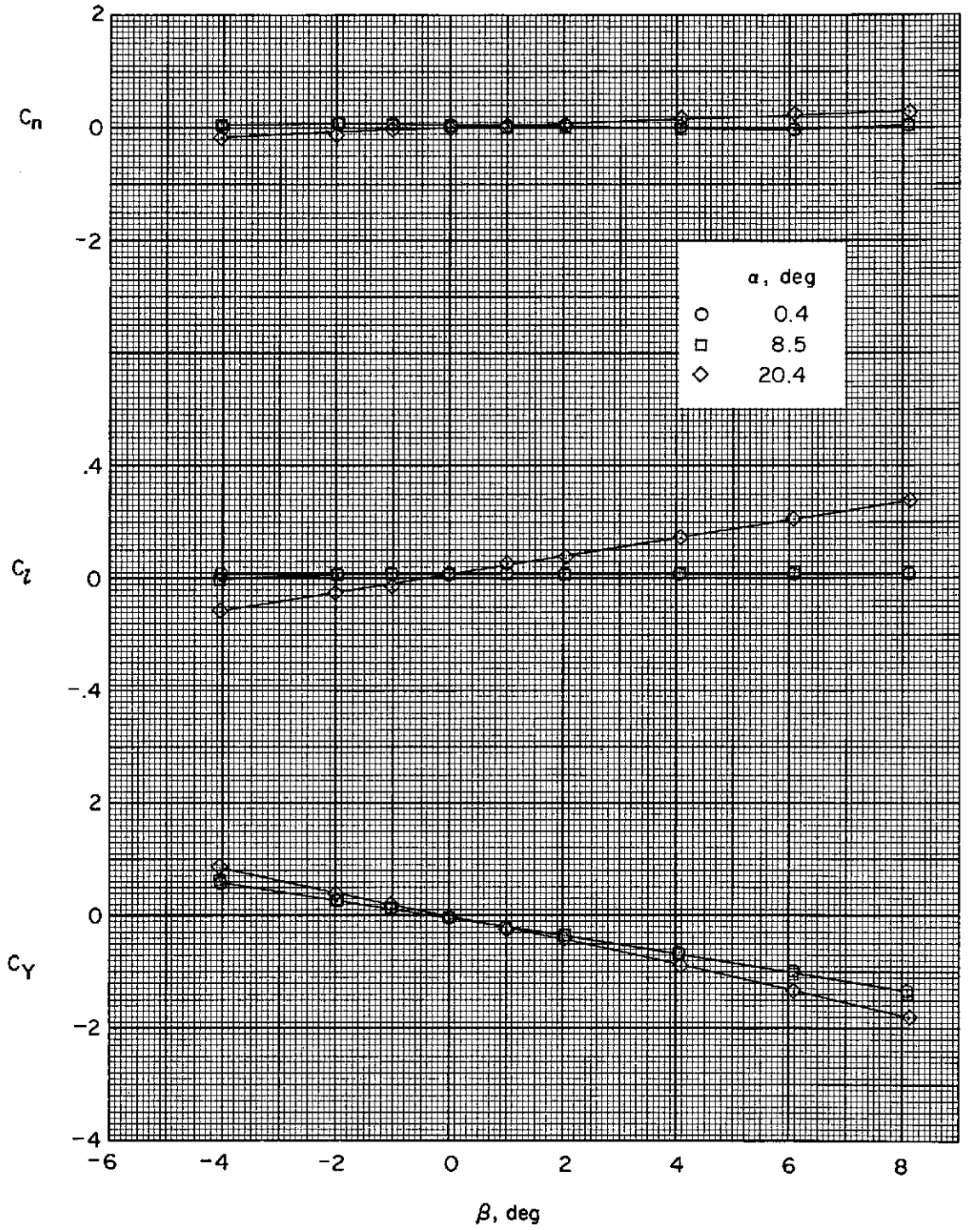

(b) Concluded.

Figure 17.- Concluded.

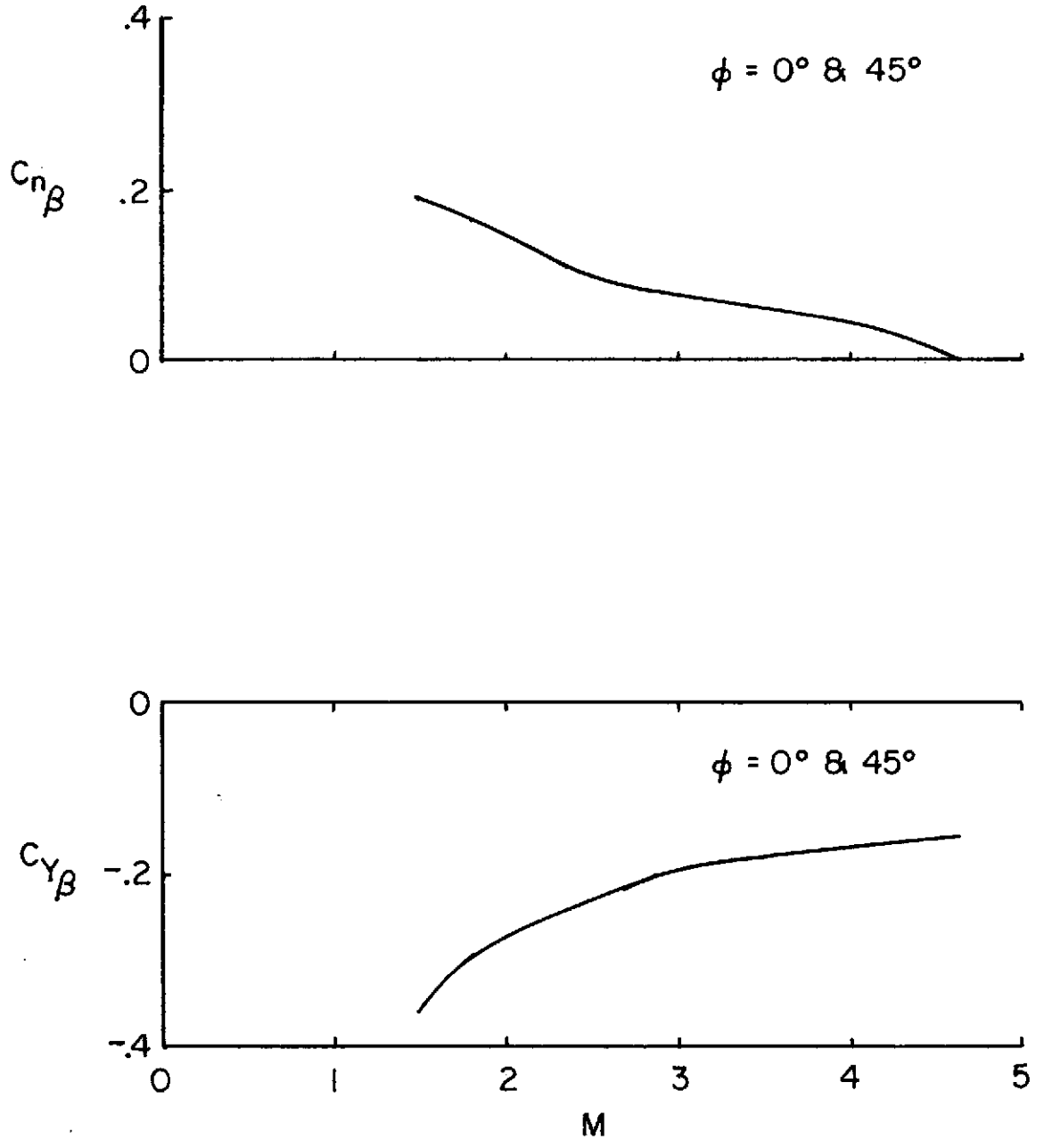

Figure 18.- Variation of sideslip derivatives with Mach number; $\alpha = 0^0$.